MISCELLANEOUS PAPER N-69-2

MINE SHAFT SERIES
EVENTS MINE UNDER AND MINE ORE
EJECTA STUDIES

by

J. W. Meyer
A. D. Rooke, Jr.

September 1969

Sponsored by

Defense Atomic Support Agency

Conducted by

U. S. Army Engineer Waterways Experiment Station
CORPS OF ENGINEERS
Vicksburg, Mississippi

ARMY-MRC VICKSBURG, MISS.

Approved for Public Release; Distribution Unlimited

ABSTRACT

The MINE SHAFT Series is a program of high-explosive tests primarily concerned with ground-shock and cratering effects from explosions at or near the surface of a rock medium. The series is sponsored by the Defense Atomic Support Agency (DASA) as a follow-on to similar tests in soil (SNOW BALL, DISTANT PLAIN, PRAIRIE FLAT). The two major events of MINE SHAFT during 1968 were MINE UNDER and MINE ORE; both were explosions of 100-ton TNT spheres detonated in near-surface geometries and in/over a granite medium.

Studies of the crater ejecta were conducted on MINE ORE (buried one-tenth of the charge radius) with the objectives of determining the spoil density and distribution from this event, examining the role of the ejection mechanism in crater formation for this medium, and obtaining additional information on natural missile trajectories. MINE UNDER, an above-surface event, produced a spalled rubble mound and a small field of debris; this was also recorded as part of the study.

MINE ORE produced a low, irregular crater lip which extended to an average range of 47 feet from ground zero (GZ) with a maximum of roughly 90 feet. Beyond this, discrete ejecta particle size and distribution frequency decreased with increasing distance from GZ. The maximum observed range was 2,120 feet for a 1-pound natural missile

with smaller fragments found out to about 2,300 feet from GZ. Maximum ejecta ranges were observed downhill from and parallel to the main joints.

Missile ranges scaled approximately as $W^{0.3}$. The jointing system of the rock appeared to be the single most influential element in concentrating debris along certain radials, as well as in the overall distribution of debris.

PREFACE

The MINE SHAFT Series includes participation by a number of agencies under the technical direction and support of the U. S. Army Engineer Waterways Experiment Station (WES). Details of the organization for Events MINE UNDER and MINE ORE are contained in a Technical, Administrative, and Operational Plan.[1] Mr. L. F. Ingram of the Nuclear Weapons Effects Division (NWED), WES, is serving as Technical Director for the MINE SHAFT Series. The Director of Program 1 (Cratering and Ejecta Studies) is Mr. J. N. Strange, also of NWED.

Subtask N122, General Ejecta Studies, was prepared and executed during the period August-November 1968 as a part of Program 1 by Messrs. A. D. Rooke, Jr., Project Officer, and J. W. Meyer, the authors of this report. Assistance in the field was provided by Messrs. J. W. Scanlan of the WES and D. E. Stroberger of the Boeing Company. During this time Mr. G. L. Arbuthnot, Jr., was Chief of the NWED, COL Levi A. Brown was Director of the WES, and Messrs. J. B. Tiffany and F. R. Brown were Technical Directors of the WES.

---

[1] DASIAC Special Report 77-1, 1 October 1968, DASA Information and Analysis Center, General Electric Co., TEMPO, 816 State Street, Santa Barbara, California.

CONTENTS

ABSTRACT---------- 3

PREFACE---------- 5

CONVERSION FACTORS, BRITISH TO METRIC UNITS OF MEASUREMENT------- 9

CHAPTER 1 INTRODUCTION---------- 10

1.1 Background---------- 10
1.2 Objectives---------- 12
1.3 Theory---------- 13
1.4 Preshot Predictions---------- 20

CHAPTER 2 EXPERIMENTAL PROCEDURES---------- 22

2.1 Test Site---------- 22
2.2 Test Schedule and Geometry---------- 23
2.3 Weather Conditions---------- 23
2.4 Ejecta Mass Density and Distribution Sampling---------- 24
2.4.1 Ejecta Within the Crater Lip---------- 24
2.4.2 Missiles Beyond the Crater Lip---------- 25
2.4.3 Ejecta-Dust Sampling---------- 26
2.5 Missile-Trajectory Experiments---------- 28
2.5.1 Colored-Grout Columns---------- 28
2.5.2 Artificial Missiles---------- 28
2.5.3 Styrofoam Missile Traps---------- 30

CHAPTER 3 PRESENTATION OF RESULTS---------- 46

3.1 Ejecta Distribution---------- 46
3.2 Ejecta Mass Density, MINE ORE---------- 48
3.2.1 Within the Crater Lip---------- 48
3.2.2 Beyond the Crater Lip---------- 48
3.3 Missile-Trajectory Experiments, MINE ORE---------- 49
3.3.1 Artificial Missiles---------- 49
3.3.2 Colored-Grout Ejecta---------- 51
3.3.3 Styrofoam Missile Traps---------- 51
3.4 Ejecta Trap---------- 51
3.5 MINE UNDER Ejecta---------- 52

CHAPTER 4 DISCUSSION OF RESULTS, MINE ORE EVENT---------- 69

4.1 Ejecta Mass Density, Volume, and Azimuthal Distribution--- 69

4.2 Ejecta Missile Ranges---------- 71
4.3 Secondary Experimental Objectives---------- 73

CHAPTER 5 TENTATIVE CONCLUSIONS AND RECOMMENDATIONS---------- 78

5.1 Tentative Conclusions---------- 78
5.2 Recommendations---------- 79
5.2.1 Procedural Changes---------- 79
5.2.2 Postseries Analysis---------- 81

REFERENCES---------- 82

TABLES

2.1 Grout-Column Color and Bead Coding, Event MINE ORE-------- 31
2.2 Artificial Missiles, Event MINE ORE---------- 32
3.1 Ejecta Size Distribution and Mass Density Within and Adjacent to the Crater Lip, MINE ORE---------- 54
3.2 Ejecta Mass Density from Photography Stations, MINE ORE--- 55
3.3 Ejecta Mass Density in Counting and Weighing Sectors, MINE ORE---------- 56
3.4 Ejecta Mass Density as a Function of Radial Distance from GZ, MINE ORE---------- 57
3.5 Average Ejecta-Dust Density---------- 58
3.6 Average Grain-Size Distribution for Ejecta Dust---------- 59
3.7 Artificial Missile Data---------- 60
3.8 Missile Impact Data from Styrofoam Missile Traps---------- 62

FIGURES

1.1 Typical half-crater profile and nomenclature for surface or near-surface burst---------- 21
2.1 Location and vicinity maps for MINE SHAFT---------- 33
2.2 Charge geometries for Events MINE UNDER and MINE ORE------ 34
2.3 Excavation trenches through the crater lip, MINE ORE------ 35
2.4 Sieving of ejecta from the crater lip of MINE ORE at rock-crushing plant---------- 36
2.5 Ejecta sampling techniques in areas beyond the crater lip, Event MINE ORE ---------- 37
2.6 Camera grid and mount for photographing ejecta beyond the crater lip, Event MINE ORE---------- 38
2.7 Sampling ejecta in the counting and weighing sectors, Event MINE ORE---------- 39
2.8 Ejecta dust-collector pad---------- 40
2.9 Ejecta dust-collector pad layout for MINE ORE, showing sampling stations and ring designations---------- 41

2.10 Recovery of samples from ejecta dust-collector pad------- 42
2.11 Cylindrical artificial missile used in MINE ORE---------- 43
2.12 Spherical artificial missiles used in MINE ORE----------- 44
2.13 Preshot positions of artificial missiles, Event MINE ORE- 45
3.1 Ejecta distribution for the MINE ORE Event--------------- 63
3.2 Outer limit of ejecta distribution, approximate southwest quadrant of MINE ORE---------- 64
3.3 Grain-size distribution of ejecta dust, Rings A-H, MINE ORE---------- 65
3.4 Postshot positions of artificial missiles, MINE ORE------ 66
3.5 Postshot positions of colored-grout ejecta, MINE ORE----- 67
3.6 MINE UNDER ejecta distribution, showing a partial plane-table survey of the larger (diameter ≧1 foot) natural missiles and other periphery of missiles at least 1 pound in weight----------
4.1 Areal mass density of ejecta as a function of distance from GZ, Event MINE ORE---------- 75
4.2 Rock-joint faces which affected MINE ORE ejecta distribution---------- 76
4.3 Isodensity contours, MINE ORE ---------- 77

CONVERSION FACTORS, BRITISH TO METRIC UNITS OF MEASUREMENT

British units of measurement used in this report can be converted to metric units as follows.

Multiply	By	To Obtain
inches	2.54	centimeters
feet	0.3048	meters
miles	1.609344	kilometers
feet per second	0.3048	meters per second
miles per hour	1.609344	kilometers per hour
square feet	0.092903	square meters
cubic yards	0.764555	cubic meters
pounds	0.45359237	kilograms
tons (2,000 pounds)	907.185	kilograms
pounds per square inch	0.070307	kilograms per square centimeter
pounds per square foot	4.88243	kilograms per square meter
pounds per cubic foot	16.0185	kilograms per cubic meter
Fahrenheit degrees	-[a]	Centigrade or Kelvin degrees

[a] To obtain Centigrade (C) temperature readings from Fahrenheit (F) readings, use the following formula: $C = (5/9)(F - 32)$. To obtain Kelvin (K) readings, use: $K = (5/9)(F - 32) + 273.15$.

CHAPTER 1

INTRODUCTION

1.1 BACKGROUND

The past 15 years or so have seen a great increase in interest and research effort on the subject of cratering. The military importance of cratering, particularly by nuclear energy, stems from its damaging capability against hardened underground facilities, from damage associated with ejected material (either in the form of impact damage or from the depth of deposition), and from the creation of tactical obstacles. Proper usage of cratering as a military tool and appreciation of its hazards require detailed knowledge of the mechanics of crater formation.

An obvious mechanism is that of ejection of material from the crater void. The early cratering tests, largely buried explosions in the arid soil of the western U. S. A., indicated that this ejection (or throwout) manifested itself primarily as an overburden problem, with areal density decreasing exponentially with increasing distance from ground zero (GZ). The small-grain material of the cratered medium posed no particular threat to nearby structures other than to render them ineffective by covering them with a blanket of soil; further, the average particle reached terminal velocity early in the ejection process, and therefore had a relatively short range.

In recent years, interest in hardened military facilities built in rock has required that additional emphasis be placed upon the study of crater ejecta in this medium. Here the possibility of long-range damage by discrete ejecta particles is as much a concern as depth-of-ejecta considerations. Further, important changes have occurred in research concepts relating to the shot geometry itself. The surface or near-surface burst, such as might be expected from an incoming warhead, has received special attention. The hemispherical charge, which sought to model the blast effects of a true surface shot (half above, half below ground) twice its actual size, has given way to the spherical charge, which more realistically represents the "point source" of energy that a nuclear burst would provide. The use of chemical explosives has, of course, been made necessary by the requirement to substitute high explosives (HE) for nuclear devices, in keeping with requirements of the Nuclear Test-Ban Treaty.[1] In addition, means have been sought to more closely reproduce the crater of a nuclear weapon, recognizing that unless this aspect of energy expenditure can be modeled it is unlikely that other aspects will be properly modeled. This has been attempted by offsetting the charge

---

[1] Entered into by the USSR, Great Britain, and the U. S. A. in 1963. Radioactive contamination of the atmosphere beyond national borders is prohibited.

center of gravity above that of the nuclear burst which is being modeled. Thus, in earlier tests in soil, it appeared that a spherical HE charge resting on (tangent to) the ground surface might provide a better representation of a nuclear surface-burst crater than one in which the center of gravity was actually at the ground surface.

It was this last consideration that dictated the choice of charge geometry for Event MINE ORE. This shot, together with the above-surface shot MINE UNDER, was a major event of the MINE SHAFT Series, a program of HE tests in rock sponsored by the Defense Atomic Support Agency. A small-scale (calibration) series of shots pointed to a burial depth of one-tenth the charge radius as most representative of a nuclear surface burst. This was generally in keeping with theoretical considerations and small-scale laboratory experiments conducted by Physics International, Incorporated.

1.2 OBJECTIVES

The primary objective of the study reported herein was to determine the ejecta mass density and azimuthal distribution associated with the MINE ORE Event. Secondary objectives were to:

1. Obtain information on the mechanics of crater formation for the MINE ORE test geometry by locating the original and final positions of ejected material.

2. Obtain information from which quantitative estimates of ejecta trajectories might be made.

3. Evaluate the hazards of natural missiles resulting from such explosions.

1.3 THEORY

The crater, lip, and surrounding regions of deformation or damage resulting from a surface or near-surface explosion are illustrated in Figure 1.1.

Preshot predictions of ejecta parameters (e.g., maximum missile range) followed two general approaches, viz, a consideration of initial particle velocities based upon shock conditions, and scaling of other experimental results to the yield for MINE ORE. The limitations on both approaches are well recognized. In the case of the former, the behavior of the shock front in the region where ejection originates is argumentative and to some extent a matter for conjecture. On the other hand, scaling of any phenomenon requires a knowledge of the mechanics involved, and these, too, are not completely understood. Thus, it is not known whether refraction of the compressive stress wave in the rock or stress relief (rebound) following the passage of the compressive stress wave predominates in the ejection mechanism. Equally uncertain is the degree to which scouring action by the explosion gases influences debris ejection. It is

likely that all of these mechanisms, among others perhaps, play a part.

Observations of near-surface explosions show an early, fast-moving "ring" of material ejected from a position near the charge and at an angle nearly normal to the ground surface, perhaps the result of a spalling action. The ejection process is, however, known to take place over a longer period of time and to include lower exit angles. This suggests that material fractured by the compressive stress wave may be dislodged and ejected by the explosion gases. In order to obtain some appreciation of the probable hazard from ejected rock, both shock conditions and scaling parameters were examined.

For the former approach, an expression for particle velocity just behind the shock front may be obtained from

$$p = \rho c u \tag{1.1}$$

where

p = shock front pressure in terms of force per unit area

ρ = medium mass density (MT^2L^{-4} in units of mass-length-time)

c = sonic velocity in the medium

u = particle velocity of the medium

Certain assumptions are immediately necessary, the major one being the value to be assigned to p. A thorough study of ejecta from a 20-ton[2] surface burst in soil (Reference 1) has shown that the

longest range particles originate near the ground surface and within a distance equal to about one charge radius from the surface of the explosive. The rock in intimate contact with the charge is probably pulverized. Material adjacent to the charge achieves large initial velocities; however, the material ejected from this region is thought to reach an early terminal velocity and experience a short trajectory, due to its highly comminuted condition. Photographic analysis indicates that this is the case (Reference 2). At a distance of around two charge radii from GZ, larger particles should remain intact. At this range, the shock wave in rock, assuming the pressure at the charge-medium interface is between 100 to 150 kilobars and decreases inversely as the square of radial distance, should be on the order of 25 to 38 kilobars. As would be expected, this is appreciably higher than comparable shock-wave pressures of about 20 kilobars observed in soil (Reference 3). Although the ground may be moving downward due to airblast loading, it is assumed that this has no significant effect on the directly coupled shock in the region of interest.

Rounding off all values to the greatest accuracy justified and solving for u,

---

[2] A table of factors for converting British units of measurement to metric units is presented on page 9.

$$u \approx \frac{(5.4 \times 10^7 \text{ lb/ft}^2)}{\left(5.0 \frac{\text{lb-sec}^2}{\text{ft}^4}\right)(1.2 \times 10^4 \text{ ft/sec})}$$

$$\approx 900 \text{ ft/sec}$$

based upon a charge-medium interface pressure of 100 kilobars. Since there is some inertia associated with all fragments, this value is actually too high. It provides, however, a point of departure for calculations of ballistic trajectory, and, further, agrees fairly well with values calculated in Reference 1 for an explosion in soil.

The equation for ballistic trajectory is well known. It states

$$R = C\left(\frac{V_o^2 \sin 2\alpha}{g}\right) \qquad (1.2)$$

where

R = range

V_o = initial velocity (speed and direction) of a projectile (or particle)

α = initial angle (with a horizontal plane) of the particle

g = gravitational acceleration

C = a constant which compensates for the effects of air drag. Reference 4, which includes some observations of ejecta particles, expresses this constant as a ratio of the observed range to the range in a vacuum.

The concept of the retarding force on an ejected particle being constant is a rather gross simplification of the actual problem, which includes such variables as particle size, shape, and velocity,

as well as density and viscosity of the air (References 4 and 5). The airblast also influences ejecta motion (Reference 6).

Substituting the calculated particle velocity for V_o in Equation 1.2, and applying certain data from Reference 1,

$$R \approx 0.05 \left[\frac{(900 \text{ ft/sec})^2 \sin 2 (25 \text{ degrees})}{32.2 \text{ ft/sec}^2} \right]$$

$$\approx 960 \text{ ft}$$

If spall is considered the predominant means of particle ejection, it may be noted that the spall velocity is twice that of the particle velocity given in Equation 1.1, or approximately 1,800 ft/sec. Substituting this value in the ballistic trajectory equation provides a range of approximately 3,860 feet. Greater ranges would result from an increase in the angle of ejection (up to 45 degrees), as might be expected for a spalled particle.

Since the results of a 1,000-pound calibration series[3] (Reference 7) were available, the selection of a suitable scaling exponent was required in order to predict certain debris parameters

---

[3] Conducted to assist in selection of a shot geometry, and also to permit the trial of certain instrumentation techniques. Charges were fired which modeled both MINE ORE and MINE UNDER, as well as other geometries in the near-surface regime.

by scaling the observed data to the yield of the MINE ORE Event. The most logical exponent appeared to be that derived from the expression for particle velocity for a buried explosion (Reference 8). With this selection, it remained to be determined which scaling rule is most applicable. Clearly, gravity must be included, which narrows the choice to mass-gravity or energy-gravity rules, as defined and developed in Reference 8. Since the former does not permit realistic scaling of linear dimensions of the charge and crater, mass-gravity scaling was tentatively chosen.

From the dimensional analysis of Reference 8, the following mass-gravity relation can readily be obtained:

$$\frac{\rho_1 u_1^2}{\rho_2 u_2^2} = \frac{g_1}{g_2}\left(\frac{\rho_1}{\rho_2}\right)^{2/3}\left(\frac{W_1}{W_2}\right)^{1/3} \tag{1.3}$$

where W is the charge weight and the subscripts 1 and 2 refer to different experiments. When ρ and g are held constant between two experiments, Equation 1.3 becomes

$$\frac{u_1}{u_2} = \left(\frac{W_1}{W_2}\right)^{1/6} \tag{1.4}$$

provided all other conditions for similarity are met. This, of course, was not the case. Yield strength, viscosity, and sonic velocity of the medium were also constant (or approximately so) in the MINE SHAFT experiments, as was hydrostatic (atmospheric) pressure. Scaling of these variables is necessary for similarity, and

failure to meet this requirement can be expected to cause deviations in what might otherwise appear to be theoretically correct scaling relations. As is pointed out in Reference 8, the cumulative result of these dissimilarities is to enlarge the scaled dimension of the larger explosion. Thus,

$$\frac{R_1}{R_2} = \left(\frac{W_1}{W_2}\right)^{1/6(+)} \qquad (1.5)$$

for the MINE SHAFT Series. If the maximum observed missile range (450 feet) for the calibration test which modeled MINE ORE is substituted in Equation 1.5, the maximum range for ejecta on MINE ORE is found to be equal to or greater than 1,200 feet.

Some experimental corroboration of the $(W)^{1/6}$ scaling rule is desirable, and this is found in Reference 9, in which it was concluded that the available maximum-range data for buried charges did indeed scale most closely to the sixth root of the charge yield. However, special attention was given to surface-burst data (taken to include hemispherical shots), for which four-tenths scaling was indicated. The latter rule provides an ejecta-range prediction on the order of 3,700 feet when applied to MINE ORE, using the calibration data as a model.

Summarizing the theoretical approaches to the determination of debris range, it appears that predictions which assume a scouring action by the shock wave are unreasonably low. Similarly,

predictions based upon sixth-root scaling are lower than would be dictated by experience. Empirically derived scaling exponents indicate a radical change in scaling associated with a surface-burst geometry. This, in turn, indicates that the sixth-root rule may become invalid as the charge position is moved upward through the earth-air interface. Why this should be is not immediately clear, since the parameters included in the dimensional analysis of Reference 8 appear equally valid for the near-surface case. Obviously, more information is needed to correlate theoretical calculations with observed results. It is particularly important that ejecta origins be determined, along with the trajectory time-histories resulting from use of various missile shapes and sizes.

1.4 PRESHOT PREDICTIONS

Based on the preceding discussion, the following preshot estimates of natural missile ranges were made for Event MINE ORE (Reference 10):

Maximum range = 3,000 feet

Range within which 90 percent of the ejecta will fall = 1,300 feet

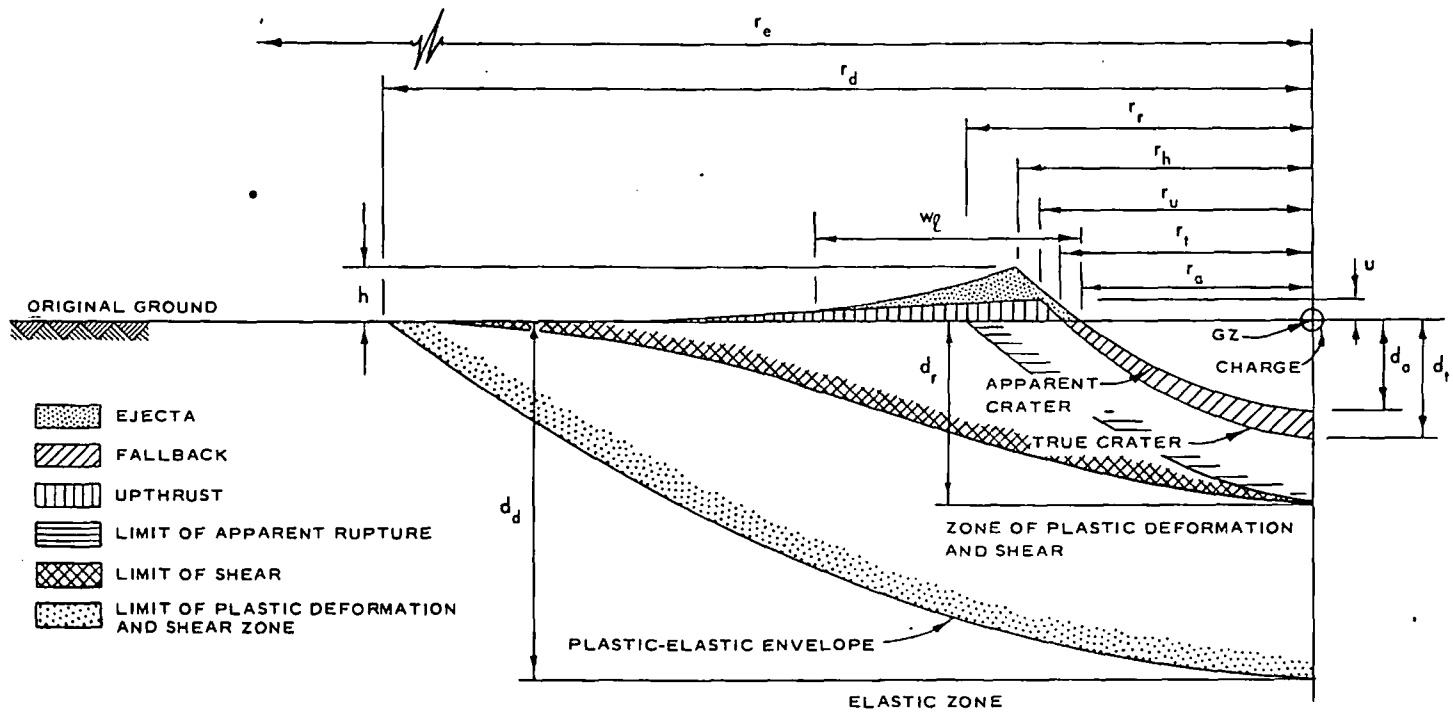

Figure 1.1 Typical half-crater profile and nomenclature for surface or near-surface burst. Profiles and dimensions are symmetrical about the centerline. Various radial and depth dimensions are indicated by r and d, respectively. Crater lip and upthrust heights are shown by h and u, while the width of the lip is noted as w_ℓ. The radius of ejected debris is indicated by r_e.

CHAPTER 2

EXPERIMENTAL PROCEDURES

2.1 TEST SITE

The MINE SHAFT test site was located on a granite laccolith in the Iron Mountains of southwest Utah, about 8 miles northwest of Cedar City, Utah. Figure 2.1 is a map of the test area. The site has a semidesert environment with juniper trees, sage, and cactus as the predominant vegetation. It is characterized by a thin layer of sandy silt soil (desert alluvium) with intermittent, smoothly rounded rock outcrops. The elevation of the site is approximately 5,900 feet msl, and the area slopes gently toward the east at about two degrees. A steep-sided, 500-foot peak is located 1,800 feet southwest of the site. The area within approximately 100 feet of both GZ's was cleared of soil and weathered rock. The trees and brush on the south and southwest sides of the area were removed for a distance of 1,000 feet from MINE ORE GZ.

The events reported herein were fired at the following geographical coordinates:

Event	Latitude	Longitude
MINE UNDER	37°46'10.050"	113°10'48.494"
MINE ORE	37°46'10.247"	113°10'49.976"

2.2 TEST SCHEDULE AND GEOMETRY

This phase of the MINE SHAFT Series consisted of two 100-ton HE charges: MINE UNDER, detonated on 22 October 1968, and MINE ORE, detonated on 13 November 1968. Each charge was formed of 32.6-pound blocks of trinitrotoluene (TNT) stacked to approximate a sphere. The charge radius was approximately 8 feet. MINE UNDER was designed as an above-surface burst with a height of burst (HOB) of 2.0 charge radii (15.70 feet). MINE ORE was a near-surface burst with an HOB of 0.9 charge radius (7.07 feet). Figure 2.2 shows the charge geometries for MINE UNDER and MINE ORE.

2.3 WEATHER CONDITIONS

Pertinent surface-weather data for MINE UNDER and MINE ORE shot days are given below:

	MINE UNDER	MINE ORE
Temperature	65.4 F	38.5 F
Barometric pressure	820 mb	808 mb
Relative humidity	18 pct	50 pct
Wind direction/velocity	300 degrees/2.3 mph	10 degrees/13.8 mph

These data were furnished by Program 5, Airblast.

2.4 EJECTA MASS DENSITY AND DISTRIBUTION SAMPLING

This section deals with the procedures for sampling the ejecta from Event MINE ORE. Since no ejecta was expected from Event MINE UNDER, the procedures discussed in the remainder of this chapter were prepared only for MINE ORE.

Measurements of ejecta mass density (pounds per square foot) were divided into three categories: (1) ejecta within the crater lip, (2) natural missiles falling beyond the crater lip, and (3) fine-grain ejecta dust falling beyond the crater lip. Primary sampling sectors extended south and west, or approximately parallel and perpendicular to what appeared to be the main jointing system of the rock.

2.4.1 Ejecta Within the Crater Lip. The mass density of the ejected material in the crater lip was determined by excavation, sieving, and weighing. Excavation was carried out in coordination with Subtask N121, Crater Investigations. Five trenches were excavated through the crater lip as shown in Figure 2.3. The trenches to the south, west, and northwest were 20-degree sectors, while those to the east and north were 6-foot-wide corridors. Each trench was divided into three sections so that mass density as a function of radial distance could be determined. The limits of these sections were spaced at one, two, and three apparent crater radii. The ejected material from each section was picked up with a front-end

loader and placed in a dump truck. The total sample was weighed, then hauled to a rock-crushing plant for sieving (Figure 2.4). There it was separated into four size groups: 12-inch plus, 6 to 12 inches, 3 to 6 inches, and 3-inch minus. Each size group was then weighed in order to provide a size-distribution curve for the specified area.

2.4.2 Missiles Beyond the Crater Lip. The number of natural rock missiles that fell beyond the crater lip were sampled three ways: (1) by photography, (2) by counting and weighing in surveyed sectors, and (3) by plane-table survey. Each method was used in a different region as shown in Figure 2.5. The objectives of this sampling were to determine mass density and a particle count per unit area of the ejecta as functions of radial distance and to examine the relation between missile size and range.

Photography was used in the region extending from 100 feet, assumed as the approximate edge of the crater lip, to 1,000 feet from GZ. Twenty photography stations, spaced to match a geometric progression, were used along both the south and west radials. The camera grid and mount used are shown in Figure 2.6. A Kodak 35-mm Reflex camera was used with Kodak Panatomic X film. The grid area covered by a single photograph was 25 ft^2. The grid pattern consisted of 6-inch squares. For those stations between 100 and 250 feet from GZ, a single photograph was taken. Between 250 and

500 feet, four photographs were taken, giving a sample area of 100 ft^2. Sixteen photographs for a sample area of 400 ft^2 were taken between 500 and 1,000 feet from GZ.

Beyond 1,000 feet from GZ, the missile population was so sparse that photography was no longer effective. Here, 20-degree counting and weighing sectors were laid out on the south and west radials as shown in Figure 2.5. Each sector was 100 feet deep. All missiles greater than 1 pound in weight in a sector were located, their positions recorded using coordinates based on the near centerline corner of the sector, and their weights estimated. Larger ejecta were weighed in a sling-and-spring-scale device. Figure 2.7 shows this procedure.

The outer fringes of the ejecta distribution were sampled by means of a plane-table survey in order to determine maximum missile range. The area surveyed was a 110-degree arc southwest of GZ as shown in Figure 2.5. As in the counting sectors, the survey was restricted to missiles at least 1 pound in weight. The remainder of the ejecta-distribution periphery was inspected visually to insure that the maximum-range missile was found.

2.4.3 Ejecta-Dust Sampling. Fine-grain ejecta dust (sand size and smaller) falling beyond the crater lip was sampled with metal collector pads like that shown in Figure 2.8. Larger particles which were found on the pads were included in the sampling; these

were found mostly on the close-in rings. Primarily, however, photography was relied upon for obtaining data on the larger particles, while the pads provided data on the fine material. The pads were arranged in a circular pattern around GZ as shown in Figure 2.9. This pattern consisted of concentric rings in a geometric progression from GZ with stations at 100, 140, 190, 270, 370, 520, 720, and 1,000 feet. The inner five rings contained 16 pads each spaced every 22.5 degrees, while the outer three rings had 32 pads each spaced every 11.25 degrees. The array contained 176 pads, of which 174 were actually placed before shot MINE ORE (satisfactory locations for two pads could not be found). Each pad was a 3- by 2.5-foot sheet of No. 20 gauge steel. The leading edge of each pad was turned down in order to anchor it more firmly into the soil overburden. Most pads were held down by 8-inch gutter spikes driven into the overburden. Some pads, located on bare rock, were held down with rock studs. The pads on the inner three rings had their leading edges anchored in grout to prevent displacement by the airblast. After the detonation, the deposited material was collected from the pads with whisk brooms and dust pans and sealed in paint cans (Figure 2.10). After an initial weighing of each sample, they were sent to the U. S. Army Engineer Waterways Experiment Station for sieve analysis.

2.5 MISSILE-TRAJECTORY EXPERIMENTS

This section describes the experiments performed to obtain data on missile-trajectory parameters such as ejection angle, initial velocity, impact angle, impact velocity, and range. Three experiments were performed involving: (1) colored-grout columns, (2) artificial missiles, and (3) styrofoam missile traps.

2.5.1 Colored-Grout Columns. An array of 8-inch boreholes was drilled in the vicinity of the MINE ORE GZ as part of the Crater Investigations Subtask (Reference 11) to aid in defining the true crater boundary and to measure residual ground displacement. One borehole was drilled at GZ, and others were drilled along radials to the south and west at 5-foot intervals. These were filled with colored grout designed to match as closely as possible the density of the granite at the test site. Portions of the columns falling within the expected area of the true crater were also divided into 1-foot sections by the addition of colored plastic beads to the grout mixture. Table 2.1 gives the coding for the colored-grout columns. After the detonation, a search was made for ejected grout particles; those located provided initial and final positions for individual pieces of crater ejecta. This provided information necessary for studying the mechanics of crater formation as well as missile trajectory.

2.5.2 Artificial Missiles. A second missile study involved

placing a large number of artificial missiles near the MINE ORE GZ. As with the grout columns, initial and final positions of the ejected material were known; however, with the artificial missiles, shape and weight were also known. This information provides a basis for studying drag forces and ballistic coefficients of discrete ejecta particles.

Two types of artificial missiles were used--cylinders and spheres. Table 2.2 lists the number of missiles placed along with their physical properties. The cylinders were made of aluminum with a 2.5-inch diameter (Figure 2.11). Each cylinder was subdivided into a 4-inch cylinder, a 2-inch cylinder, a 1-inch cylinder, and a 1-inch cylinder divided into half and quarter wedges (see Table 2.2). The cylinders were emplaced in NX holes (3-inch diameter) at 2.5 and 7.5 feet from GZ along the south and west radials. The spherical missiles were made of three metals: aluminum, steel, and lead (Figure 2.12). They varied from 1 to 6 inches in diameter. The missiles were number-coded and placed in the two NX holes and in the top 3 feet of the first five grout holes (excluding GZ) along the south radial. Figure 2.13 shows the preshot positions of the artificial missiles. Density-matching grout was used to backfill around the missiles.

Seven large aluminum missiles were also used in an attempt to evaluate initial trajectory conditions of ejecta. It was planned

that with their brightly polished or painted surfaces they would be detected by the test photography, giving early velocity data (ejection angle and speed).

2.5.3 Styrofoam Missile Traps. Styrofoam missile traps were used to evaluate terminal trajectory parameters. The traps were 8- by 4-foot styrofoam pads (125-psi compressive strength), 4 inches thick. Six such pads were used along a radial to the south of GZ (Figure 2.9) at distances of 400, 500, 600, 700, 800, and 900 feet. Each pad was positioned so that its top surface was flush with the ground surface. After the detonation, the pads were examined for missile hits from which impact angles and depths of penetration could be measured. From these values it is anticipated that the impact velocities of the missile can be inferred by calibration experiments relating penetration and impact velocity.

TABLE 2.1 GROUT-COLUMN COLOR AND BEAD CODING, EVENT MINE ORE

Material above dashed line was dissociated and/or ejected. Holes R1-1 through R1-5 also contained artificial missiles (see Figure 2.13). Key to bead colors: R, red; Y, yellow; T, turquoise; A, amber; Bl, black; O, orange; G, green.

Column→	GZ	R1-1	R1-2	R1-3	R1-4	R1-5	R1-6	R1-7	R1-8	R1-9
Grout Color→	Red	Brown	Green	Black	Yellow	Orange	Brown	Green	Red	Yellow
Range, feet→	0	5	10	15	20	25	30	35	40	45
Depth	Bead Color(s)									
feet										
South Radial (Azimuth = 195 degrees):										
0-1	R	T	Y	R	R,Y	O	R	T	T	T
1-2	G	Y	A	O	G	Bl	Y	Y	Y	G
2-3	T	O	G	G	T	A	O	O	O	A
3-4	Y	Bl	R	T	Y	T	Bl	G	Bl	R
4-5	T	A	T,Y	A	O	R	T	R	--	Bl
5-6	A	R,G	T,O	Bl,T	A	R,T	G	A	--	--
6-7	Bl	R,T	T,Bl	R,G	R,G	T,A	--	--	--	--
7-8	R,G	R,Y	--	R,A	R,T	Bl,T	--	--	--	--
8-9	R,T	R,O	--	--	R	--	--	--	--	--
9-10	R,Y	R,Bl	--	--	--	--	--	--	--	--
10-11	R,O	R,A	--	--	--	--	--	--	--	--
11-12	R,Bl	--	--	--	--	--	--	--	--	--
12-13	R,A	--	--	--	--	--	--	--	--	--

Column→	R3-1	R3-2	R3-3	R3-4	R3-5	R3-6	R3-7	R3-8	R3-9
Grout Color→	Black	Orange	Yellow	Green	Black	Brown	Red	Yellow	Black
Range, feet→	5	10	15	20	25	30	35	40	45
Depth	Bead Color(s)								
feet									
West Radial (Azimuth = 279 degrees):									
0-1	T	A	T	R	T	R	A	T	A
1-2	R	R	Y	G	G	G	R	Y	R
2-3	G	T	G,A	T	Y	O	T	C	Y
3-4	Y	G	Bl	Y	O	T	G	G	G
4-5	Bl	Y	O	O	Bl	Bl	--	--	--
5-6	O	Bl	A	Bl	A	A	--	--	--
6-7	A	O	G	A	G	--	--	--	--
7-8	T,R	R,A	R	R,G	R	--	--	--	--
8-9	T,G	R,O	R,A	R,T	T,Y	--	--	--	--
9-10	T,Y	R,Bl	T,A	--	O,Bl	--	--	--	--
10-11	T,Bl	R,Y	Bl,A	--	--	--	--	--	--
11-12	T,O	R,G	--	--	--	--	--	--	--
12-13	T,A	R,T	--	--	--	--	--	--	--

TABLE 2.2 ARTIFICIAL MISSILES, EVENT MINE ORE

Missile Type	Material	Size		Weight	Number Emplaced
		Length	Diameter		
		inches	inches	pounds	
Cylinder	Aluminum	4	2.5	1.82	39
Cylinder	Aluminum	2	2.5	0.91	39
Cylinder	Aluminum	1	2.5	0.46	39
Cylinder	Aluminum	1[a]	--	0.23	39
Cylinder	Aluminum	1[b]	--	0.12	78
Sphere	Aluminum	--	6.0	10.50	5
Sphere	Aluminum	--	5.5	8.10	2
Sphere	Aluminum	--	2.5	0.76	26
Sphere	Aluminum	--	1.0	0.05	114
Sphere	Lead	--	2.5	3.37	24
Sphere	Steel	--	2.0	1.17	8
Sphere	Steel	--	1.0	0.15	10
				Total	423

[a] Cylinder divided into half wedges.
[b] Cylinder divided into quarter wedges.

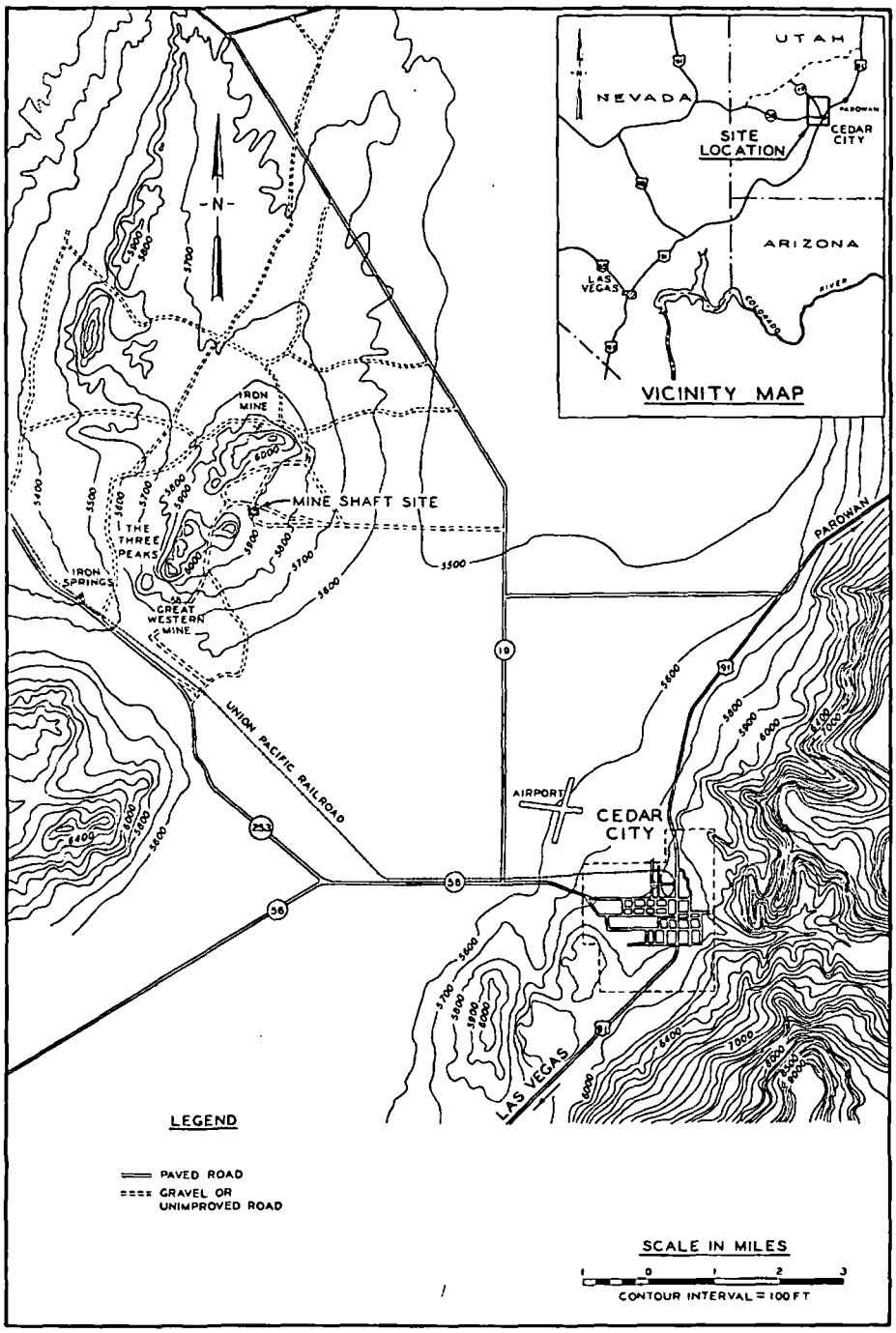

Figure 2.1 Location and vicinity maps for MINE SHAFT. Contours are in feet above mean sea level (msl).

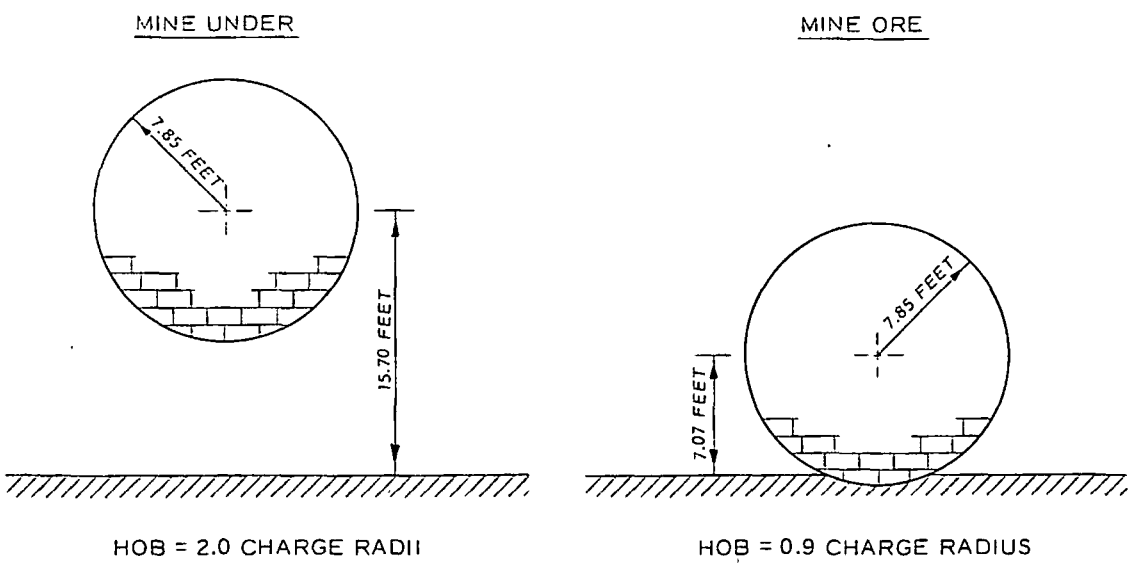

Figure 2.2 Charge geometries for Events MINE UNDER and MINE ORE.

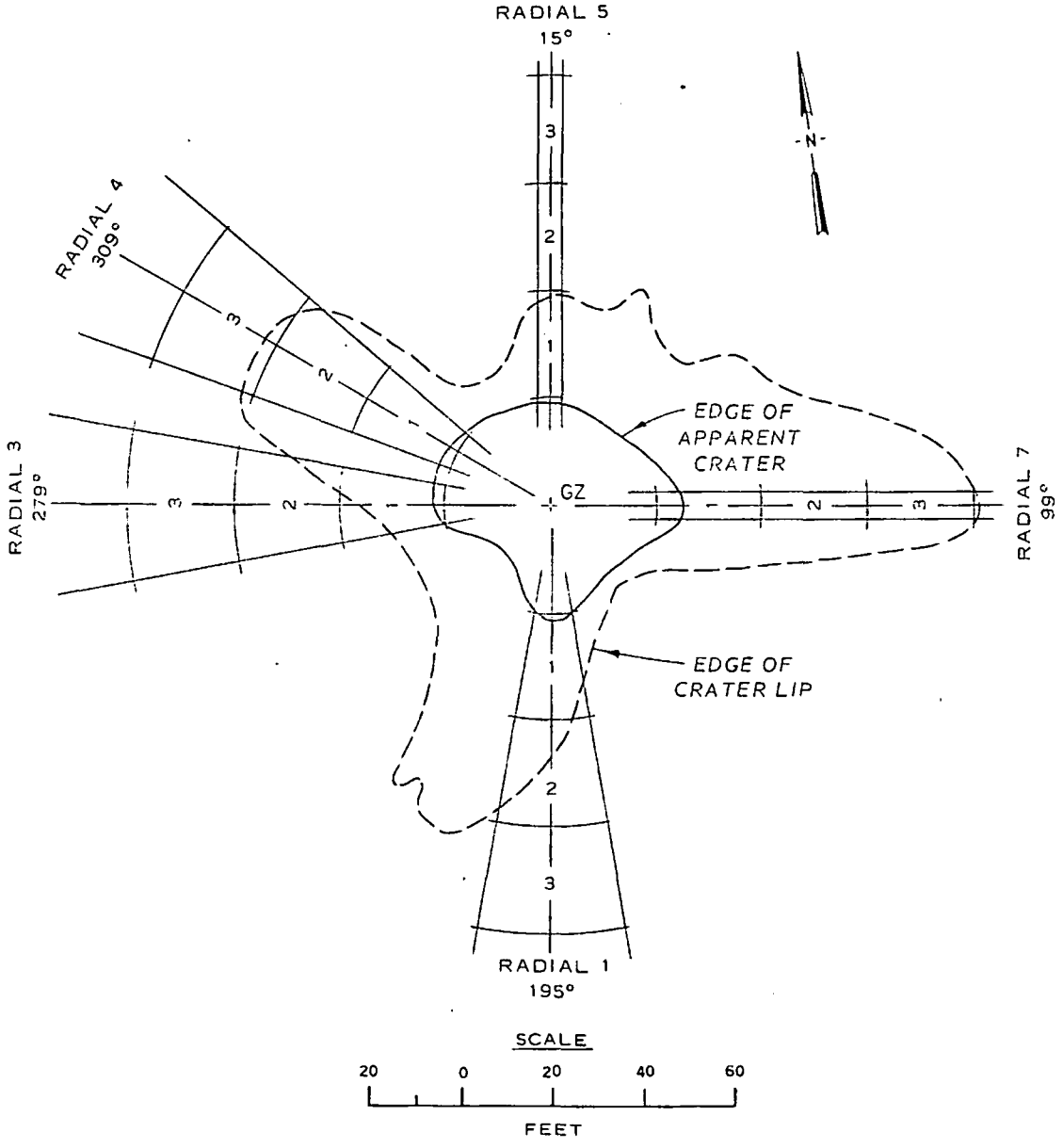

Figure 2.3 Excavation trenches through the crater lip, MINE ORE. Radial numbering system corresponds with that of Crater Investigations Study (Subtask N121). Arrow indicates true north.

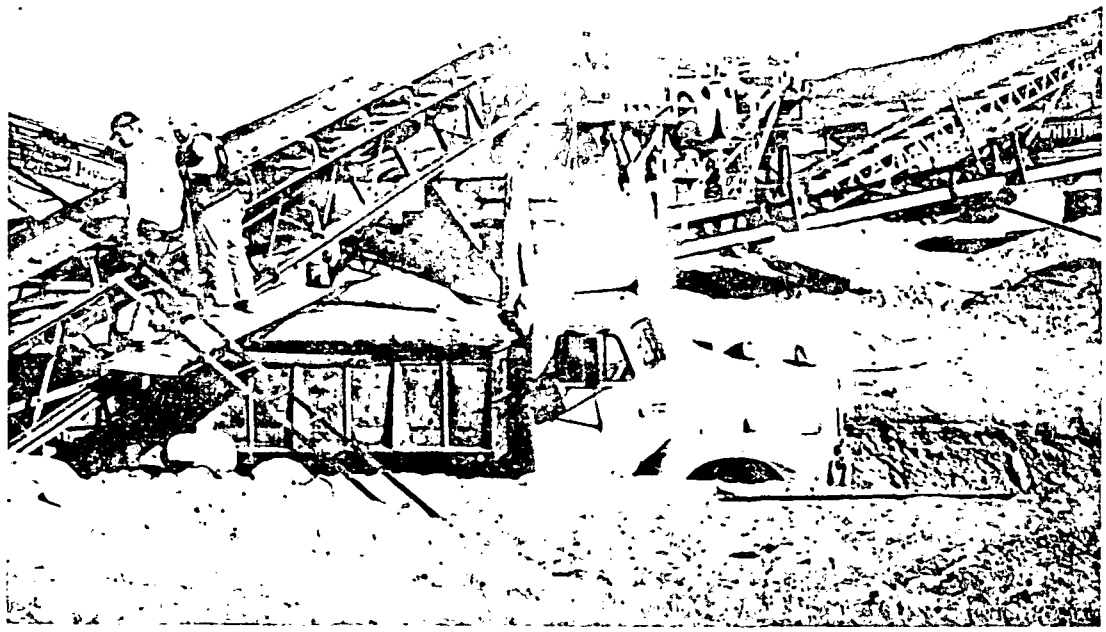

Figure 2.4 Sieving of ejecta from the crater lip of MINE ORE at rock-crushing plant (Western Rock Products Corp., Cedar City, Utah).

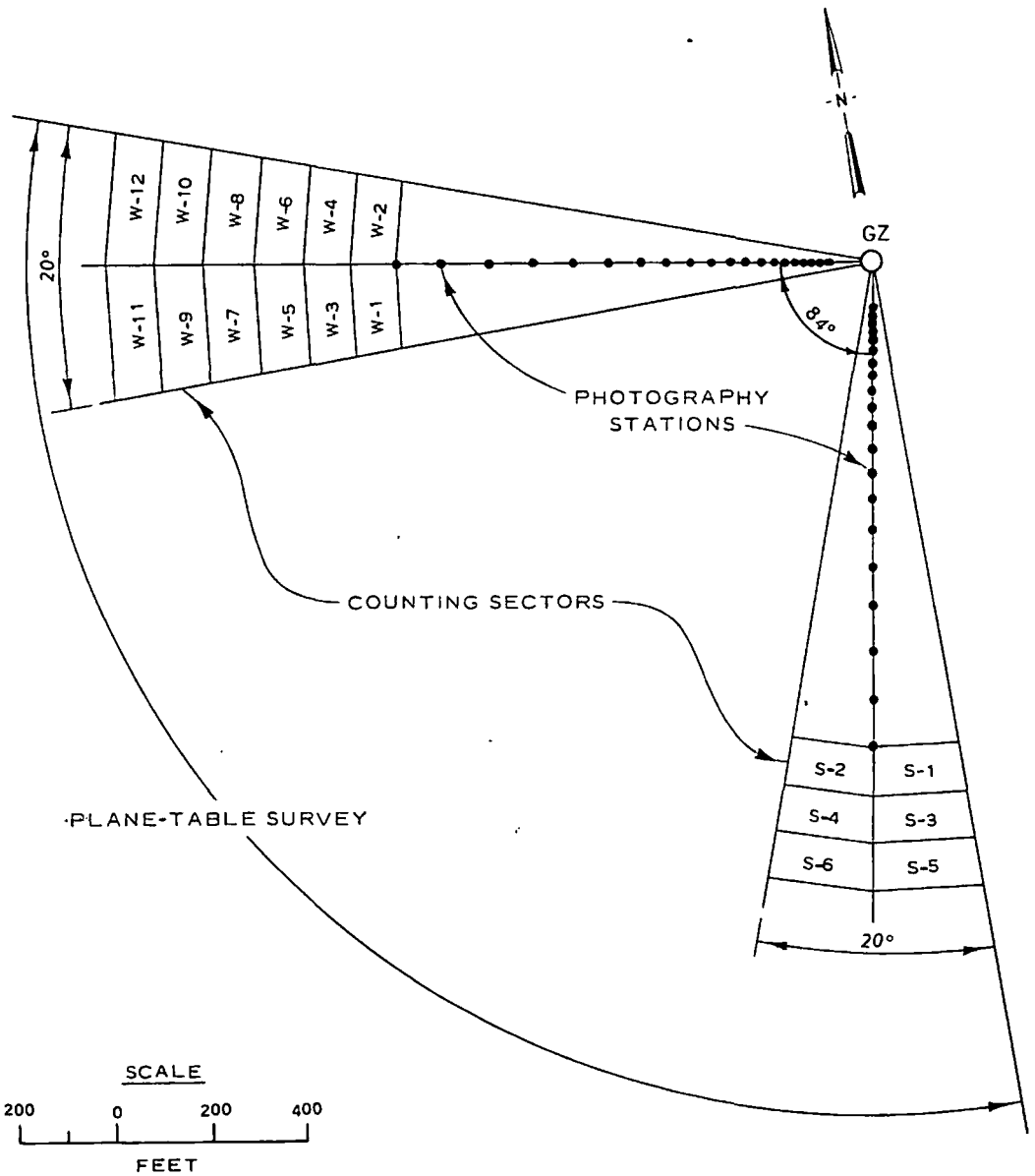

Figure 2.5 Ejecta sampling zones in areas beyond the crater lip, Event MINE ORE.

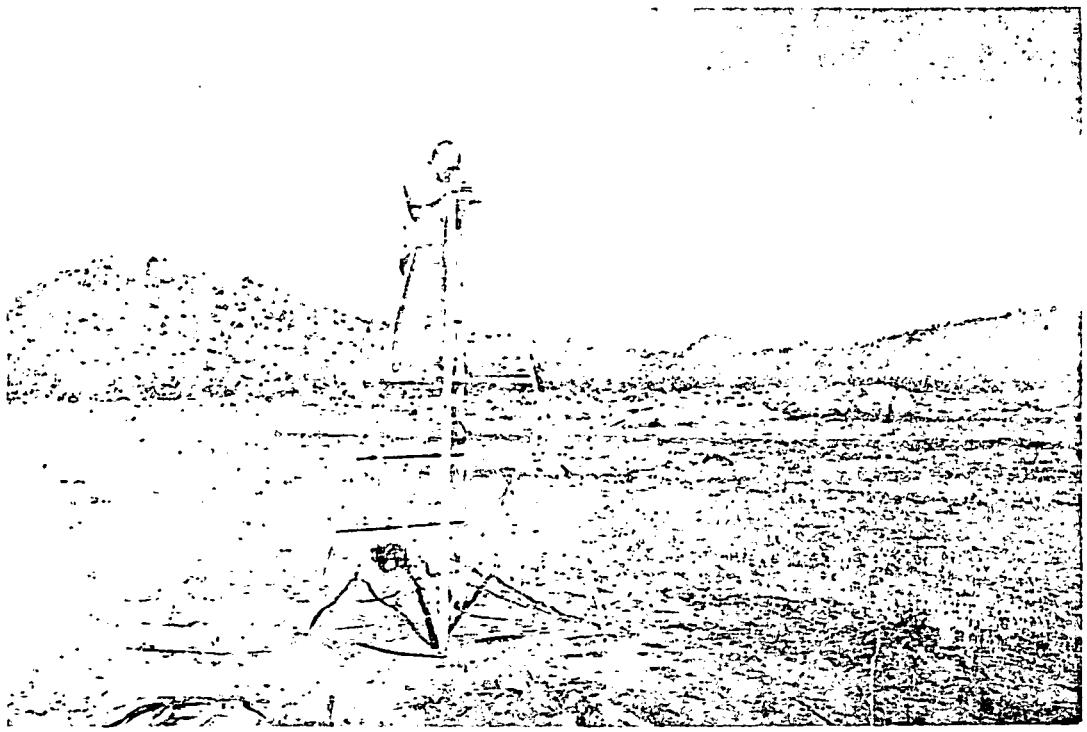

Figure 2.6 Camera grid and mount for photographing ejecta beyond the crater lip, Event MINE ORE.

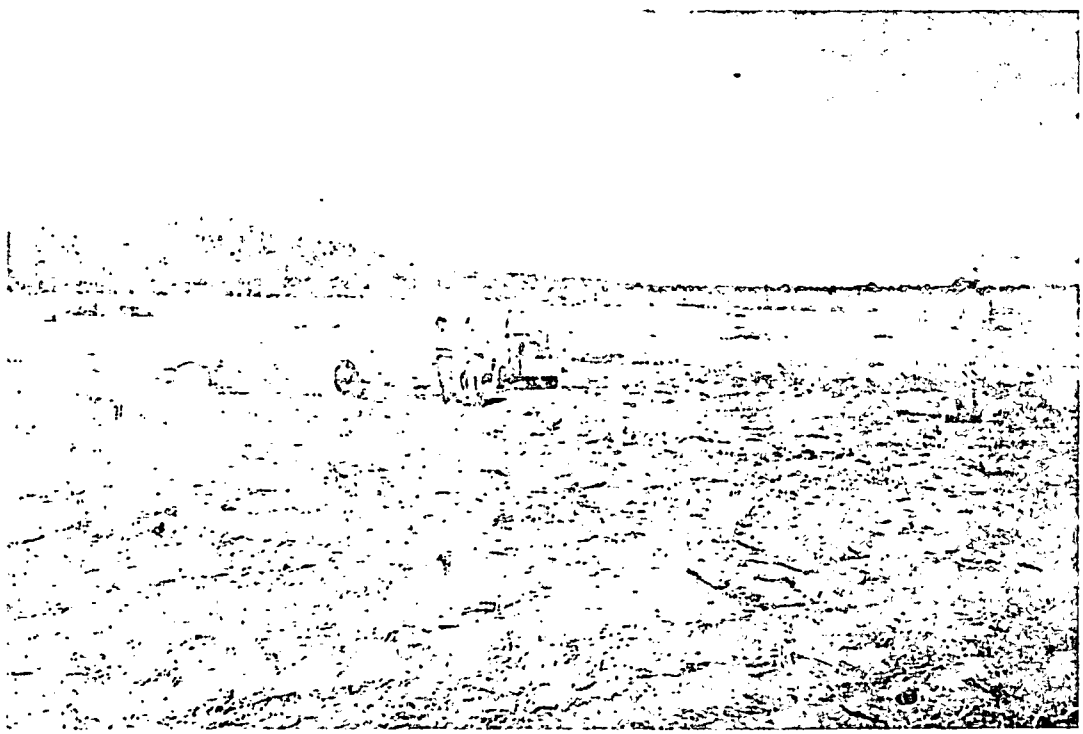

Figure 2.7 Sampling ejecta in the counting and weighing sectors, Event MINE ORE. GZ is in the background at left. Spring scale can be seen near truck.

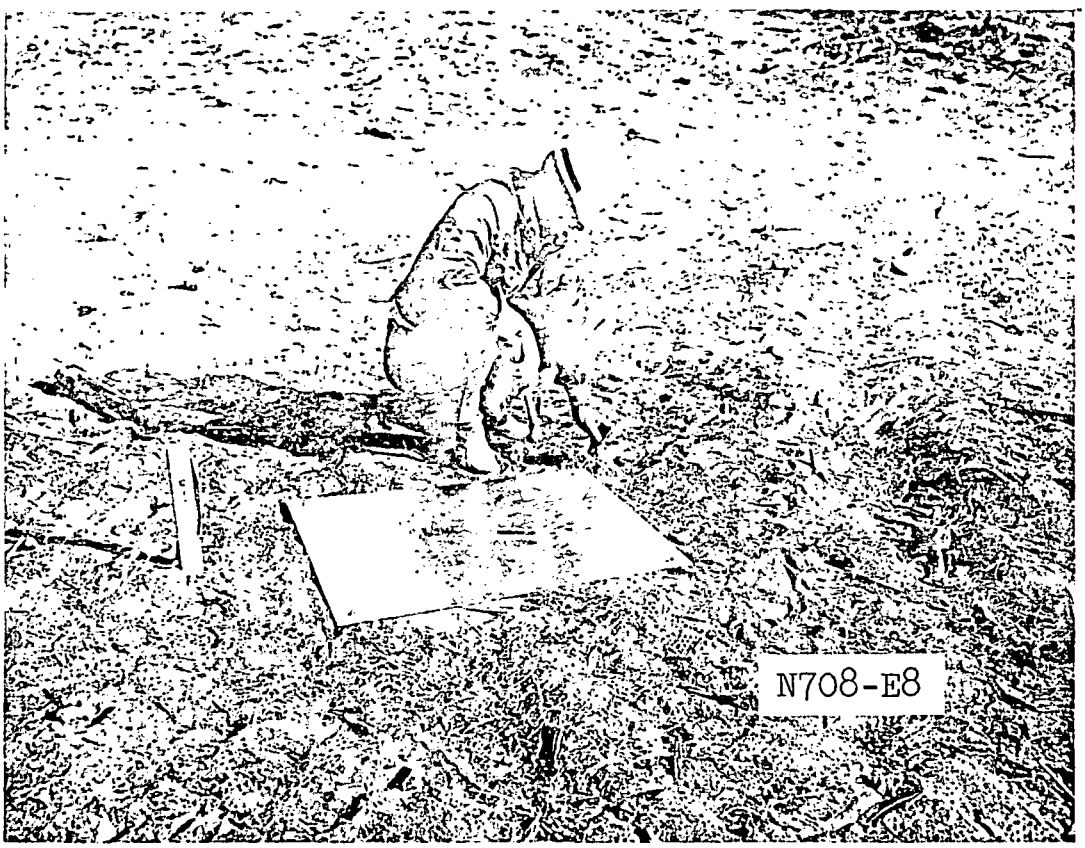

Figure 2.8 Ejecta dust-collector pad.

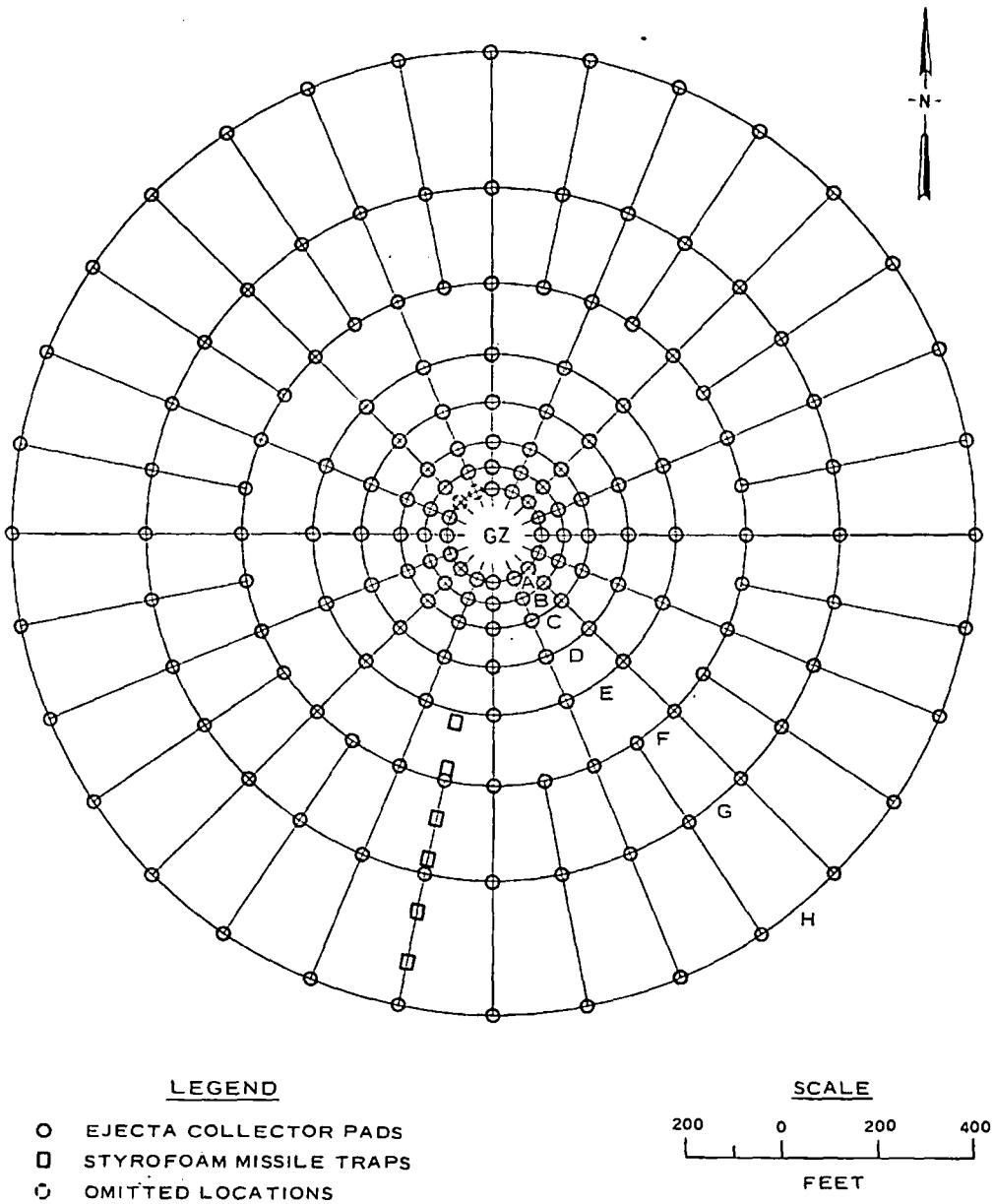

Figure 2.9 Ejecta dust-collector pad layout for MINE ORE, showing sampling stations and ring designations.

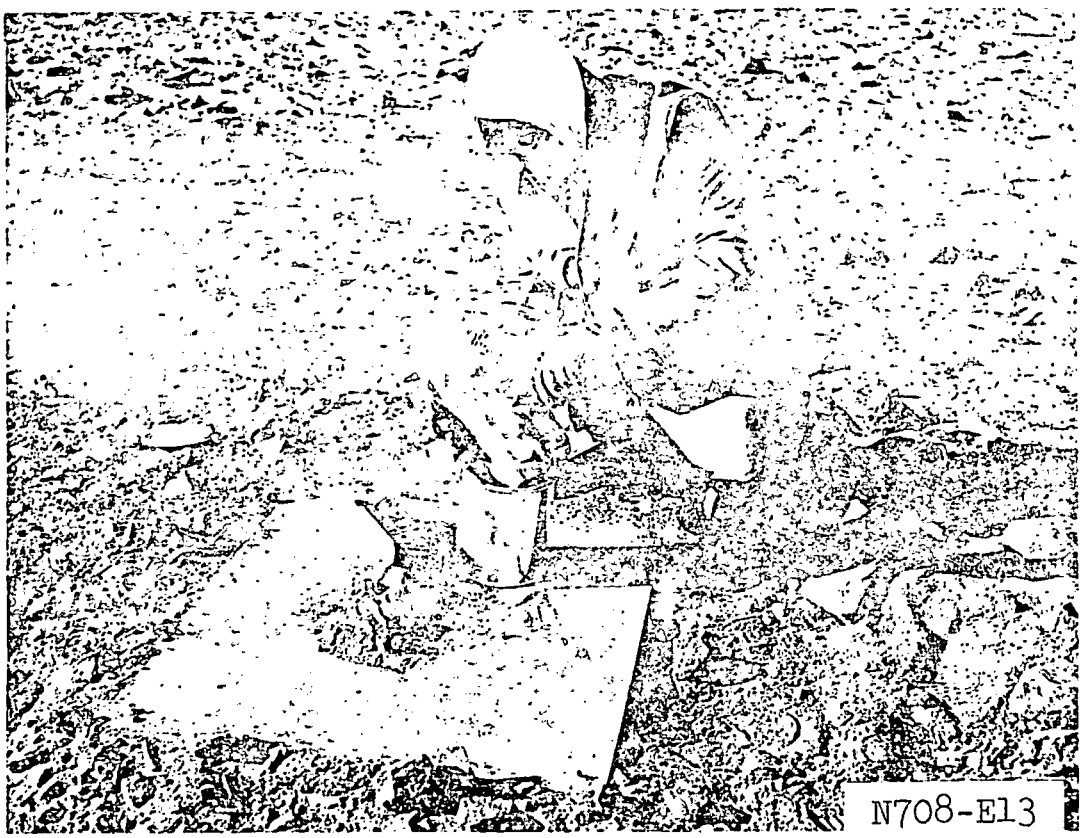

Figure 2.10 Recovery of samples from ejecta dust-collector pad.

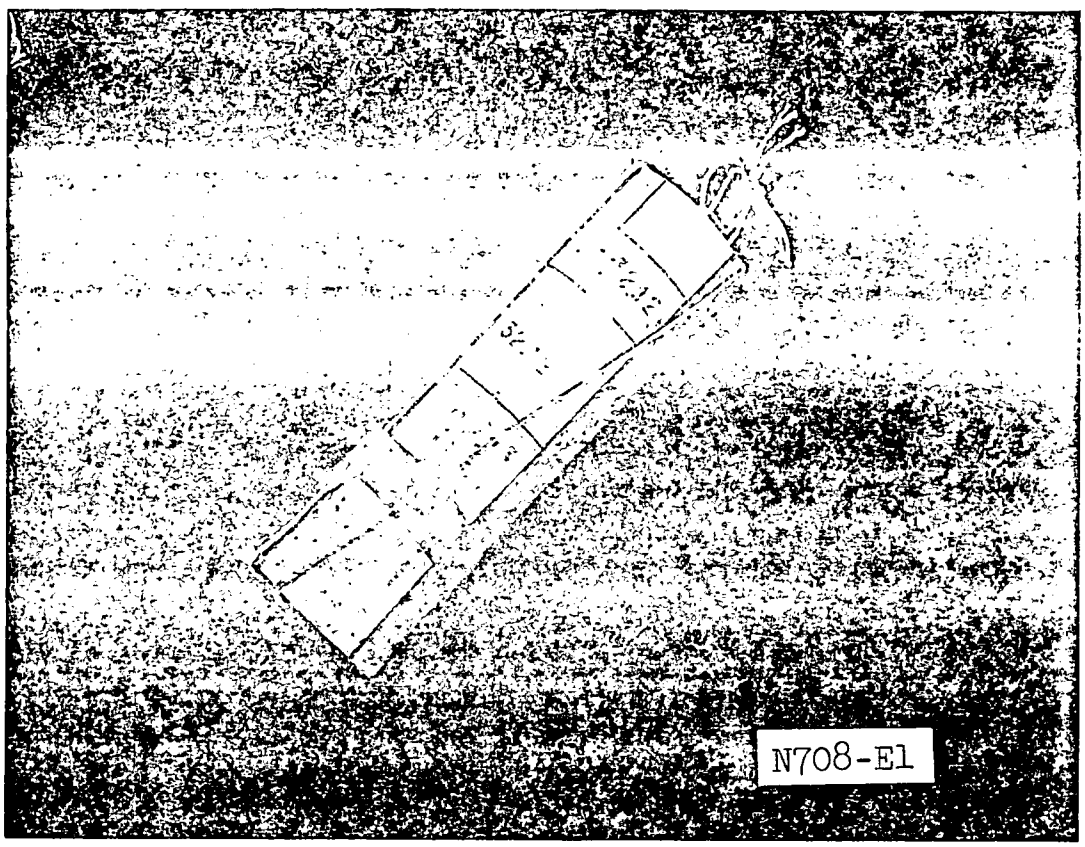

Figure 2.11 Cylindrical artificial missile used in MINE ORE.

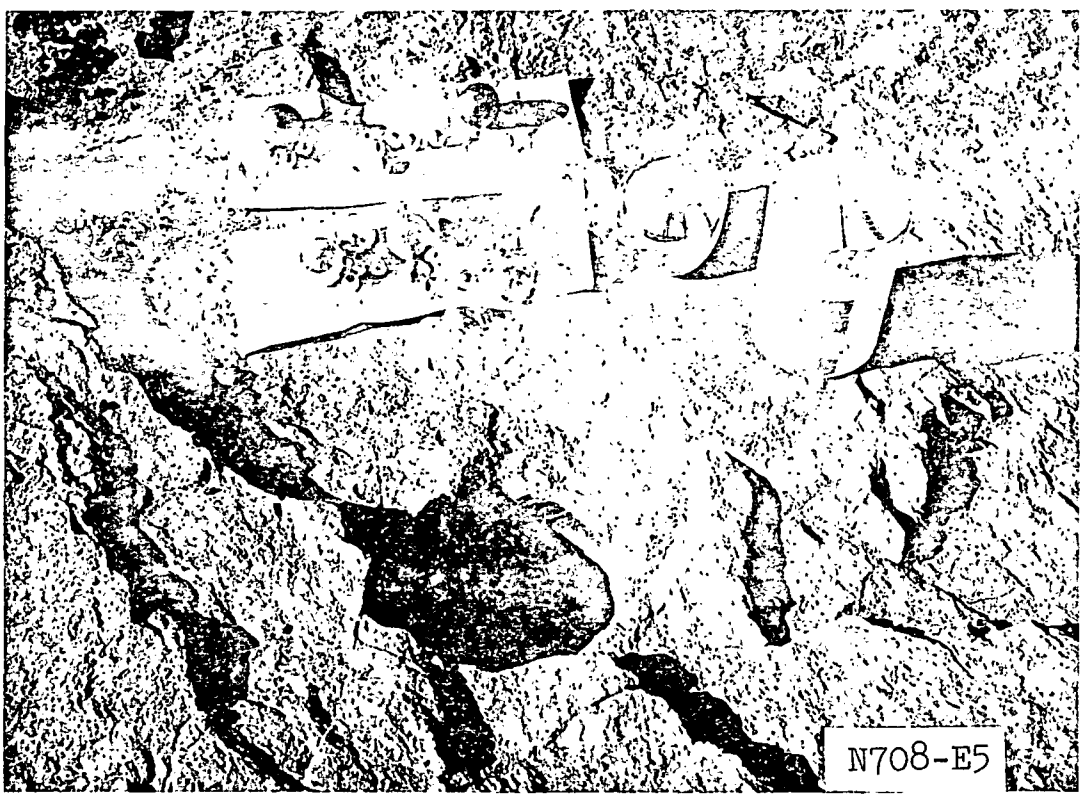

Figure 2.12 Spherical artificial missiles used in MINE ORE. Missile at right is encased in plaster of paris.

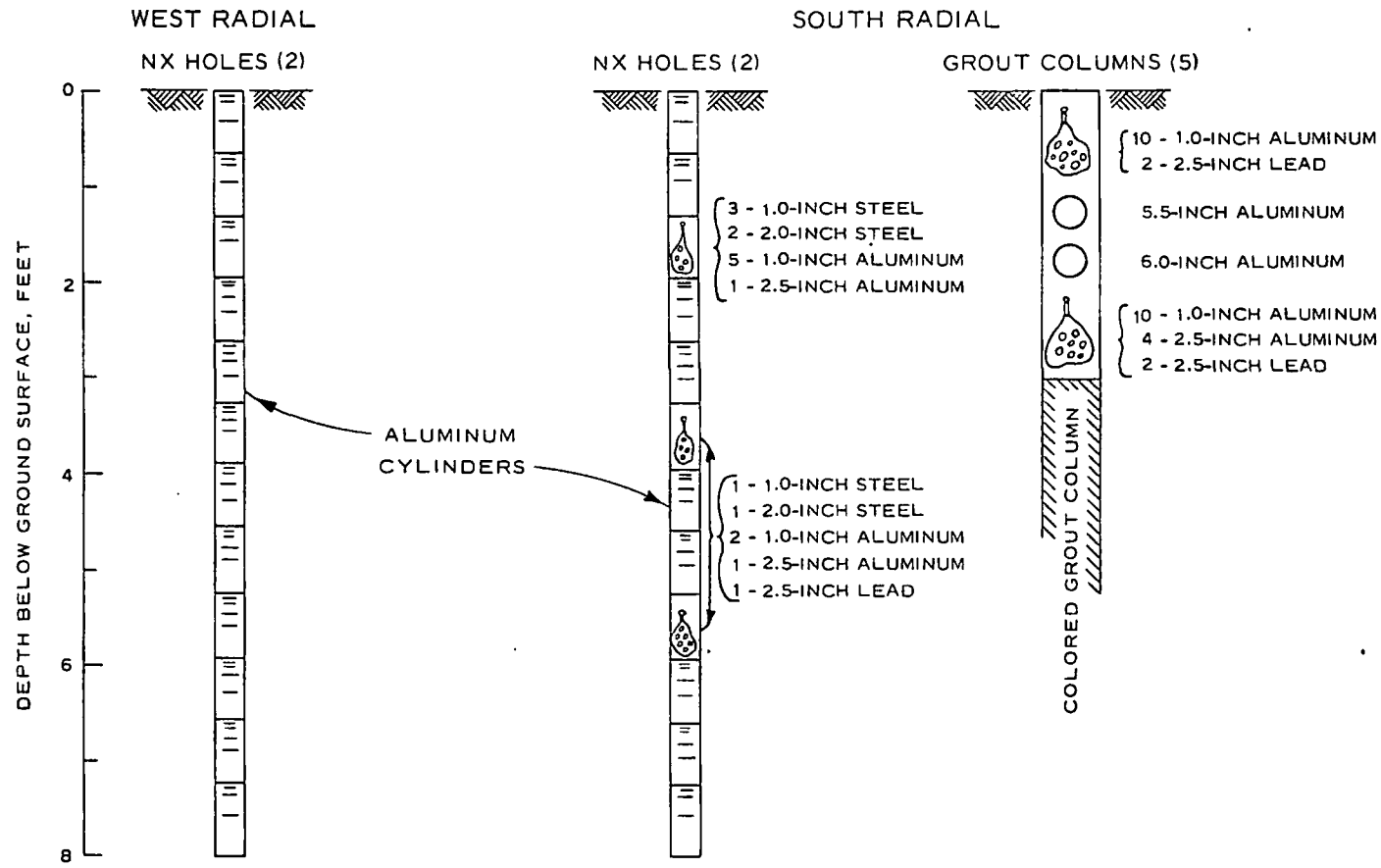

Figure 2.13 Preshot positions of artificial missiles, Event MINE ORE.

CHAPTER 3

PRESENTATION OF RESULTS

3.1 EJECTA DISTRIBUTION

Figure 3.1 is a postshot aerial photograph of the MINE ORE site showing the ejecta distribution pattern. Several distinct ejecta rays are visible, extending northwest, south-southwest, south, and east. The formation of these rays appeared to be controlled by the vertical joint faces found in the rock mass in the vicinity of GZ (Reference 11), the joint faces tending to deflect and channel a large portion of the ejecta along these rays. Between rays, distribution of discrete ejecta appeared to be random and less dense. The northwest ejecta ray was taken as typical and examined in some detail. It was found to be approximately 950 feet long. The numerical density of the missiles remained fairly constant at 10 to 12 missiles per square foot. However, the average size of the missiles (and thus the mass density) decreased with increasing distance from GZ. A few large missiles, greater than 1 foot in diameter, were found in the ray. Again, the frequency decreased with increased distance from GZ.

Although the jointing pattern of the rock was probably the single most important factor in the ejecta distribution (apart from test conditions of yield, medium, and geometry), other topographical and

vegetal features of the test site were also influential. The site sloped gently to the south and east at about 2 degrees, with missile ranges being greater in the downhill direction. A large hill was located approximately 1,800 feet west-southwest of GZ, restricting somewhat missile ranges in that direction. To the south of GZ, juniper and pine trees were removed to a distance of only 1,000 feet from GZ. Since missile ejection angles were small due to the high center of gravity of the charge geometry and there was evidence of considerable bounce and roll with accompanying comminution, these trees had a screening effect which reduced the range of missiles because of their flat trajectories.

Ambient wind conditions had no visible effect on the distribution of the discrete ejecta. The only part of the experiment subject to weather disturbance was the dust samples on the metal collector pads. However, the majority of these samples were collected immediately after the shot (within 6 hours), before they could be disturbed significantly by wind. The weather in the 2-week data collection period following the shot was cool but fair.

Maximum significant missile range for MINE ORE was 2,120 feet for a 1-pound missile lying south-southeast of GZ. A few smaller particles were noted 100 to 200 feet farther from GZ, giving a maximum range of about 2,300 feet. Figure 3.2 is a plane-table map of the long-range natural missiles in the southwest quadrant. The

maximum-range missiles were found downslope of GZ and roughly parallel to the main north-south jointing pattern of the rock. In other directions, the approximate periphery of missile distribution was as follows: north--1,600 feet; east--1,800 feet.

3.2 EJECTA MASS DENSITY, MINE ORE

3.2.1 Within the Crater Lip. Table 3.1 gives the size distribution and mass densities for the ejected material excavated from the MINE ORE crater lip. Examination of these data and Figure 2.3 shows that the ejecta was not evenly distributed around the crater, but was thickest to the east, south, and northwest. As with the missile-ejecta distribution, this distribution was probably controlled by the rock jointing system near GZ.

3.2.2 Beyond the Crater Lip. Tables 3.2 through 3.4 give the ejecta mass density beyond the crater lip. Table 3.2 contains the data from the photography stations which were used between the edge of the crater lip (100 feet from GZ) and 1,000 feet from GZ. The data include sample area, number of missiles, total ejecta weight in the area, and mass density. Table 3.3 gives the same information for the counting and weighing sectors used beyond 1,000 feet. Finally, Table 3.4 summarizes ejecta mass density, exclusive of pad samples, as a function of radial distance for the south and west radials.

The ejecta-dust density data from the metal collector pads are given in Tables 3.5 and 3.6. Samples were recovered from 152 (87 percent) of the pads. In Table 3.5, the average mass density for each ring is shown. Table 3.6 gives the average grain-size distribution for the ejecta on each ring, while Figure 3.3 presents grain-size distribution curves. The plots show that the material was mostly a uniformly graded, sand-sized alluvium. The curves for Rings A, B, and F show the influence of ejected rock missiles which landed randomly on pads in these rings.

3.3 MISSILE-TRAJECTORY EXPERIMENTS, MINE ORE

The results of the experiments designed to evaluate missile-trajectory parameters are discussed below. The tests included the artificial missiles, colored-grout column ejecta, and styrofoam missile traps.

3.3.1 Artificial Missiles. Table 3.7 presents the results of the artificial missile experiment, including only those missiles located and identified postshot. A total of 423 artificial missiles (cylinders and spheres) were emplaced preshot. Eighty-one, or 19 percent, were recovered, identified, and mapped postshot. Several other missiles were found, but they were badly deformed or too scarred to be identifiable. In Table 3.7, the identification number of each missile gives its initial position. For the cylinders, the

first digit identifies the radial on which the missile was located, the second digit gives the borehole number, and the third digit, on the right of the decimal, denotes the relative depth of that missile in the borehole. For example, Cylinder No. 31.5 was originally placed on Radial 3 (279 degrees azimuth), Borehole No. 1 (2.5 feet from GZ), and was the fifth missile down from the ground surface. Since all spheres were placed along the south radial, their identification numbers give only hole number (first digit) and nominal depth in feet (second digit). Thus, Sphere 43 was originally emplaced in Hole 4 (20 feet from GZ) at a depth of approximately 3 feet. The seven large spheres were identified by color or by a single number indicating borehole location. Figure 3.4 is a plane-table map of the postshot positions of the artificial missiles.

Most artificial missiles found had traveled less than 200 feet. Only three long-range artificial missiles were located: a 2-inch cylinder (32.2) located 1,662 feet along the west radial, an unidentified 1-inch quarter cylinder at 1,412 feet along the west radial, and a 1-inch cylinder (12.4) at 1,051 feet along the south radial. The maximum range for a sphere was 209 feet for a 1-inch aluminum sphere (41) originally located 20 feet from GZ at a depth of 0.98 foot. The large polished or painted aluminum spheres which were located traveled less than 210 feet and were not detected by the test photography.

3.3.2 Colored-Grout Ejecta. Figure 3.5 shows the postshot positions of the colored-grout ejecta. The maximum range for a piece of grout ejecta was 1,250 feet to the west of GZ. Average weight of the grout missiles was about 2 pounds. The majority of the colored-grout ejecta followed two of the ejecta rays, to the northwest and south-southwest. An analysis of initial position and range of the colored-grout ejecta in the study of crater formation is found in Reference 11.

3.3.3 Styrofoam Missile Traps. The measurements of terminal trajectory parameters obtained from the styrofoam missile traps are given in Table 3.8. The missile traps were placed too far from GZ to obtain a good sample of natural missiles. Those collected were very small, most of them being approximately 1 cm in diameter and weighing less than 1 gram. It was also noted that most had impact angles greater than 90 degrees, indicating that at the time of impact they were traveling toward GZ, evidently as a result of the negative-pressure phase and accompanying afterwinds.

3.4 EJECTA TRAP

An ejecta collector trap, installed at the request of the Boeing Company, was located about 75 feet northeast of GZ. This consisted of a 4-foot-square wooden box, placed in a natural depression in the overall rock formation. Although the depth varied

slightly across the bottom of the cavity, the average depth was about 38 inches. Sufficient grout was poured outside the box to bring the surrounding surface up to the top of the box.

The cavity was severely deformed by the blast, with only the west corner remaining intact. The east and west corners were filled with ejecta to ground level, while the north and south corners were filled to within 1.80 and 1.20 feet of ground level, respectively. The average thickness of deposition in the cavity was 2.5 feet. Since the trap was located beyond the edge of the crater lip in an area occupied only by discrete ejecta particles, this deposition indicates that a considerable amount of the material deposited had arrived by the process of rolling and bouncing along the ground surface rather than by direct missile trajectory.

3.5 MINE UNDER EJECTA

Although no crater or ejecta was expected from Event MINE UNDER, a rubble mound and some ejected material were observed after the blast. Presumably, this was the result of shallow spallation of the rock surface (possibly enhanced by pile-driving action by the wooden legs of the charge support platform) and elastic rebound. The ejecta field consisted of rock fragments thrown out in an irregular pattern around GZ. A plane-table map (Figure 3.6) was made of the larger ejecta missiles and the outer fringes of the ejecta distribution,

where the survey was restricted to missiles at least 1 pound in weight. The maximum missile range observed was 695 feet for a 1-pound missile lying northwest of GZ. The major concentration of ejecta, an oval-shaped cluster, lay approximately 250 feet southwest of GZ. Smaller concentrations were found to the southeast and north. The southeast and southwest concentrations were roughly perpendicular to a main north-south joint in the rock on the west side of GZ. These concentrations followed smaller east-west joints. The small northern concentration paralleled the main joint. However, the effect of the rock jointing on the ejecta distribution was not as evident here as it was for MINE ORE. This is presumably due to the fact that the spallation process involved only the top few inches of the rock surface and the ejecta was not subject to deflection and channeling by vertical joints as was the ejecta from MINE ORE.

TABLE 3.1 EJECTA SIZE DISTRIBUTION AND MASS DENSITY WITHIN AND ADJACENT TO THE CRATER LIP, MINE ORE

Radial	Section	Weight of Ejecta of Indicated Sizes, inches				Total Weight of Ejecta	Areal Mass Density
		>12	6-12	3-6	<3		
		pounds	pounds	pounds	pounds	pounds	lb/ft^2
1	1	16,970	4,960	7,460	7,040	36,430	132
	2, 3	4,788	1,310	4,330	4,670	15,098	14
3	1	--	--	--	--	--	--
	2	488	587	268	487	1,830	4
	3	105	205	318	546	1,174	2
4	1	--	--	--	--	--	--
	2, 3	25,360	5,300	9,190	16,220	56,070	52
5	1	5,980	1,370	2,720	3,060	13,130	95
	2	630	660	180	1,260	2,703	20
	3	150	125	109	75	459	3
7	1, 2, 3	36,470	5,710	9,620	17,860	69,660	168

TABLE 3.2 [illegible] MASS DENSITY FROM [illegible] STATIONS, MINE ORE

Distance[a] from GZ	Station[b] Area	[illegible] Missiles	Calculated Ejecta Weight	Areal Mass Density
feet	ft^2		pounds	lb/ft^2
West Radial:				
100	20	18	22.11	1.11
115	20	17	31.16	1.56
130	20	3[illegible]	[illegible]	[illegible].28 × 10^{-1}
145	20	7	6.30	3.15 × 10^{-1}
165	20	[illegible]	4.77	[illegible] × 10^{-1}
185	20	33	[illegible].13	4.57 × 10^{-1}
210	20	14	1.05	[illegible] × 10^{-2}
235	20	10	1.41	7.05 × 10^{-2}
[illegible]	72	11	[illegible]	[illegible].11 × 10^{-1}
[illegible]	72	[illegible]	[illegible]	7.[illegible] × 10^{-1}
[illegible]	72		[illegible]	7.31 × 10^{-1}
[illegible]	72	[illegible]	[illegible]	1.17 × 10^{-1}
[illegible]50	72	[illegible]	[illegible]	[illegible] × 10^{-2}
[illegible]	272	11	[illegible]	[illegible] × 10^{-2}
[illegible]	272	[illegible]	[illegible]	3.40 × 10^{-2}
710	272	11	10.1[illegible]	[illegible] × 10^{-2}
805	272	11	7.89	2.[illegible] × 10^{-2}
905	272	3	1.69	[illegible] × 10^{-3}
1,000	272	5	2.09	7.68 × 10^{-3}
South Radial:				
100	20	44	127.20	6.36
115	20	49	131.[illegible]	6.58
130	[illegible]	[illegible]3	13[illegible].6[illegible]	6.78
14[illegible]	20	26	123.82	6.19
165	20	49	145.55	7.28
185	20	43	49.55	2.48
210	20	38	131.62	6.58
235	20	22	16.63	8.32 × 10^{-1}
270	72	15	28.27	3.93 × 10^{-1}
385	72	6	13.72	1.91 × 10^{-1}
435	72	6	8.14	1.13 × 10^{-1}
490	72	2	10.35	1.44 × 10^{-1}
555	272	16	8.83	3.25 × 10^{-2}
630	272	24	12.12	4.46 × 10^{-2}
710	272	21	25.50	9.38 × 10^{-2}
805	272	16	9.64	3.54 × 10^{-2}
905	272	9	6.51	2.39 × 10^{-2}
1,000	272	23	23.65	8.69 × 10^{-2}

[a] Stations 300 and 340 on the south radial and 340 on the west radial fell within access road.

[b] Station areas reduced from actual grid size due to trimming and overlapping of photographs.

TABLE 3.3 EJECTA MASS DENSITY IN COUNTING AND WEIGHING SECTORS, MINE ORE

Sector	Distance from GZ[a]	Sector Area	No. of Missiles	Ejecta Weight	Areal Mass Density
	feet	ft^2		pounds	lb/ft^2
S-1	1,050	18,300	13	18	9.84×10^{-4}
S-2	1,050	18,300	70	162	9.40×10^{-3}
S-3	1,150	20,000	13	65	3.25×10^{-3}
S-4	1,150	20,000	29	49	2.45×10^{-3}
S-5	1,250	21,850	1	1	4.58×10^{-5}
S-6	1,250	21,850	6	12	5.49×10^{-4}
W-1	1,050	18,300	44	96	5.25×10^{-3}
W-2	1,050	15,600	6	7	4.49×10^{-4}
W-3	1,150	20,000	24	37	1.85×10^{-3}
W-4	1,150	17,450	6	7	4.01×10^{-4}
W-5	1,250	21,850	16	17	7.78×10^{-4}
W-6	1,250	19,150	5	5	2.61×10^{-4}
W-7	1,350	23,450	11	12	5.12×10^{-4}
W-8	1,350	20,850	6	7	3.36×10^{-4}
W-9	1,450	25,250	3	3	1.19×10^{-4}
W-10	1,450	22,700	5	6	2.64×10^{-4}
W-11	1,550	26,450	9	15	5.67×10^{-4}
W-12	1,550	25,550	4	6	2.35×10^{-4}

[a] To center of sector.

TABLE 3.4 EJECTA MASS DENSITY AS A FUNCTION OF RADIAL DISTANCE FROM GZ, MINE ORE

Distance from GZ	Areal Mass Density	
	West Radial	South Radial
feet	lb/ft^2	lb/ft^2
100	1.11	6.36
115	1.56	6.58
130	9.28×10^{-1}	6.78
145	3.15×10^{-1}	6.19
165	2.39×10^{-1}	7.28
185	4.57×10^{-1}	2.48
210	5.25×10^{-2}	6.58
235	7.05×10^{-2}	8.32×10^{-1}
270	5.11×10^{-2}	3.93×10^{-1}
300	7.22×10^{-1}	--
340	--	--
385	7.31×10^{-1}	1.91×10^{-1}
435	1.17×10^{-2}	1.13×10^{-1}
490	7.01×10^{-2}	1.44×10^{-1}
555	5.44×10^{-2}	3.25×10^{-2}
630	9.40×10^{-2}	4.46×10^{-2}
710	5.95×10^{-2}	9.38×10^{-2}
805	2.90×10^{-2}	3.54×10^{-2}
905	6.95×10^{-3}	2.39×10^{-2}
1,000	7.68×10^{-3}	8.69×10^{-2}
1,050	2.85×10^{-3}	5.19×10^{-3}
1,150	1.13×10^{-3}	2.85×10^{-3}
1,250	5.20×10^{-4}	2.97×10^{-4}
1,350	4.24×10^{-4}	--
1,450	1.92×10^{-4}	--
1,550	4.01×10^{-4}	--

TABLE 3.5 AVERAGE EJECTA-DUST DENSITY

Ring	Distance from GZ	Average Weight of Ejecta per Pad	Areal Mass Density
	feet	pounds	lb/ft^2
A	100	15.92	2.27
B	140	31.02	4.42
C	190	18.29	2.61
D	270	5.93	0.84
E	370	2.32	0.33
F	520	2.40	0.34
G	720	0.72	0.10
H	1,000	0.11	0.02

TABLE 3.6 AVERAGE GRAIN-SIZE DISTRIBUTION FOR EJECTA DUST

Ring	Weight of Material Retained on and Percentage of Material Finer than Indicated Sieve										
	1-inch		1/2-inch		No. 4		No. 16		No. 200		Pan
	Retained	Passing	Retained	Passing	Retained	Passing	Retained	Passing	Retained	Passing	Retained
	pounds	percent	pounds	percent	pounds	percent	pounds	percent	pounds	percent	pounds
A	5.76	63	0.58	59	0.67	55	4.09	29	3.04	10	1.60
B	8.02	73	1.19	69	1.50	64	3.08	54	11.39	15	4.30
C	2.29	87	0.30	85	0.49	82	1.84	72	9.13	21	3.79
D	0.77	88	0.15	86	0.23	82	0.81	69	3.33	16	1.05
E	0.27	88	0.05	86	0.06	83	0.27	71	1.31	15	0.37
F	1.05	52	0.02	51	0.04	49	0.19	40	0.63	11	0.27
G	0.15	80	0.01	79	0.02	76	0.09	64	0.35	17	0.12
H	0.02	80	Negli-gible	80	0.01	70	0.01	60	0.04	20	0.02

TABLE 3.7 ARTIFICIAL MISSILE DATA

Missile No.	Cylinder Length or Sphere Diameter	Initial Position			Final Position		Distance Traveled
		Radial Azimuth	Distance from GZ	Depth from Surface	Radial Azimuth	Distance from GZ	
	inches	degrees	feet	feet	degrees	feet	feet
Aluminum Cylinders, 2.5-inch Diameter:							
11.5	1[a]	195	2.5	0.60	211	19	17
11.5	1[b]	195	2.5	0.60	271	53	53
11.5	1	195	2.5	0.69	249	11	11
11.11	2	195	2.5	6.69	195	3	1
11.11	4	195	2.5	6.94	195	3	1
12.4	1	195	7.5	0.27	200	1,051	1,043
12.5	1[a]	195	7.5	0.91	213	222	215
12.5	1	195	7.5	1.00	205	257	249
12.5	2	195	7.5	1.12	194	195	237
12.5	4	195	7.5	1.37	211	57	49
12.6	1	195	7.5	2.23	215	72	65
12.6	2	195	7.5	2.35	211	74	66
12.6	4	195	7.5	2.60	203	58	55
31.2	4	279	2.5	0.78	163	42	44
31.5	4	279	2.5	2.64	208	16	16
32.2	2	279	7.5	0.39	284	1,662	1,654
32.6	2	279	7.5	3.15	269	67	59
32.6	4	279	7.5	3.40	255	90	83
32.7	1	279	7.5	3.79	256	50	43
32.8 (2)	1[a]	279	7.5	4.34	279	12	5
32.8	1[b]	279	7.5	4.34	279	12	5
32.8	1	279	7.5	4.43	279	12	5
32.9	1	279	7.5	4.96	254	10	2
Spheres:							
1	6 A[c]	195	5.0	2.13	179	33	28
3	6 A	195	15.0	1.66	194	216	201
4	6 A	195	20.0	1.24	203	132	112
5	6 A	195	25.0	1.62	192	147	122
Orange	5-1/2 A	195	15.0	2.06	193	200	185
Red	5-1/2 A	195	25.0	2.12	200	35	10
23	2-1/2 A	195	10.0	3.42	192	135	125
23	2-1/2 A	195	10.0	3.42	192	135	125
23	2-1/2 A	195	10.0	3.42	205	145	135
33	2-1/2 A	195	15.0	2.70	199	195	180
33	2-1/2 A	195	15.0	2.70	196	174	159
33	2-1/2 A	195	15.0	2.70	195	159	144
33	2-1/2 A	195	15.0	2.70	198	156	141

(Continued)

[a] Cylinder divided into quarter wedges.
[b] Cylinder divided into half wedges.
[c] A denotes aluminum; L denotes lead.

TABLE 3.7 ARTIFICIAL MISSILE DATA (CONCLUDED)

Missile No.	Cylinder Length or Sphere Diameter	Initial Position			Final Position		Distance Traveled
		Radial Azimuth	Distance from GZ	Depth from Surface	Radial Azimuth	Distance from GZ	
	inches	degrees	feet	feet	degrees	feet	feet
Spheres (Continued):							
43	2-1/2 A	195	20.0	1.61	202	134	114
43	2-1/2 A	195	20.0	1.61	207	121	102
43	2-1/2 A	195	20.0	1.61	208	92	73
53	2-1/2 A	195	25.0	4.87	202	31	6
53	2-1/2 A	195	25.0	4.87	202	31	6
53	2-1/2 A	195	25.0	4.87	202	31	6
53	2-1/2 A	195	25.0	4.87	215	37	16
21	1 A	195	10.0	2.67	193	197	187
23	1 A	195	10.0	3.42	193	133	123
23	1 A	195	10.0	3.42	193	106	96
23	1 A	195	10.0	3.42	194	170	160
31	1 A	195	15.0	1.29	195	219	204
31	1 A	195	15.0	1.29	200	206	192
31	1 A	195	15.0	1.29	193	197	182
31	1 A	195	15.0	1.29	194	187	172
33	1 A	195	15.0	2.70	199	191	176
33	1 A	195	15.0	2.70	198	178	163
33	1 A	195	15.0	2.70	194	115	100
33	1 A	195	15.0	2.70	201	114	99
33	1 A	195	15.0	2.70	199	191	176
33	1 A	195	15.0	2.70	200	152	137
41	1 A	195	20.0	0.98	199	223	203
41	1 A	195	20.0	0.98	197	229	209
41	1 A	195	20.0	0.98	197	224	204
41	1 A	195	20.0	0.98	197	224	204
41	1 A	195	20.0	0.98	201	181	161
41	1 A	195	20.0	0.98	197	165	145
41	1 A	195	20.0	0.98	197	173	153
43	1 A	195	20.0	1.61	201	103	83
43	1 A	195	20.0	1.61	208	110	90
43	1 A	195	20.0	1.61	208	110	90
53	1 A	195	25.0	4.87	215	37	16
53	1 A	195	25.0	4.87	215	37	16
53	1 A	195	25.0	4.87	215	37	16
53	1 A	195	25.0	4.87	215	37	16
53	1 A	195	25.0	4.87	215	37	16
53	1 A	195	25.0	4.87	215	37	16
53	1 A	195	25.0	4.87	215	37	16
53	1 A	195	25.0	4.87	215	37	16
31	2-1/2 L	195	15.0	1.29	193	192	177
41	2-1/2 L	195	20.0	0.98	200	184	164
43	2-1/2 L	195	20.0	1.61	207	85	65
43	2-1/2 L	195	20.0	1.61	201	102	82
53	2-1/2 L	195	25.0	4.87	215	37	16

TABLE 3.8 MISSILE IMPACT DATA FROM STYROFOAM MISSILE TRAPS

Missile No.	Distance from GZ	Missile Weight	Impact Angle[a]	Depth of Penetration
	feet	grams	degrees	feet
1	400	1.07	98.0	0.082
2	400	0.51	96.0	0.140
3	400	0.09	91.5	0.059
4	400	0.35	89.0	0.205
5	400	4.29	109.5	0.090
6	400	0.15	88.0	0.132
7	400	0.09	92.5	0.063
8	400	0.21	92.0	0.078
9	500	0.40	100.5	0.165
10	500	0.35	108.5	0.100
11	500	0.30	99.0	0.067
12	500	0.09	87.5	0.081
13	500	0.92	112.0	0.036
14	500	0.21	78.0	0.036
15	600	0.10	92.0	0.045
16	600	2.80	90.5	0.069
17	800	2.96	~100	0.070

[a] Sketch illustrating impact angle:

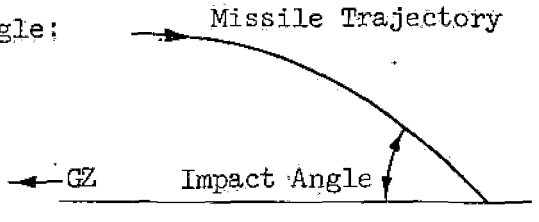

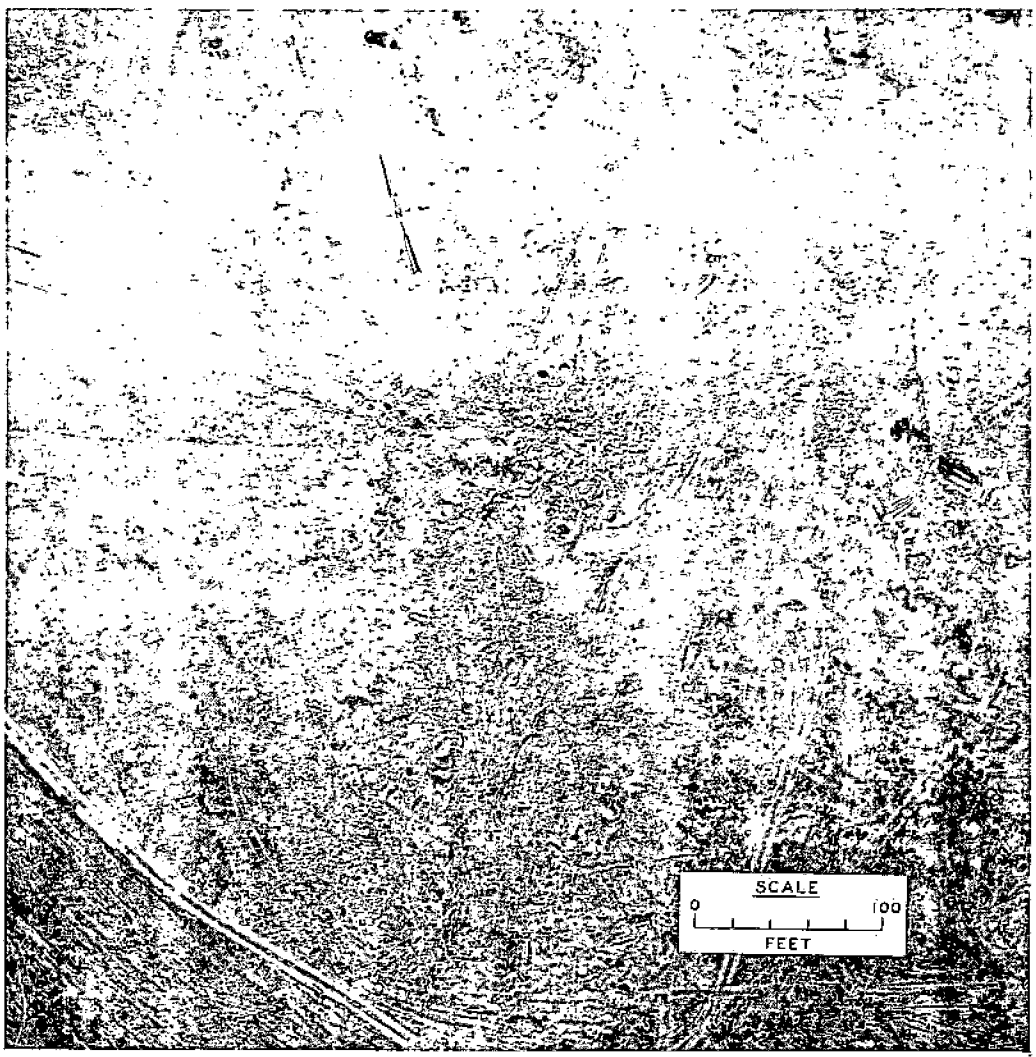

Figure 3.1 Ejecta distribution for the MINE ORE Event.

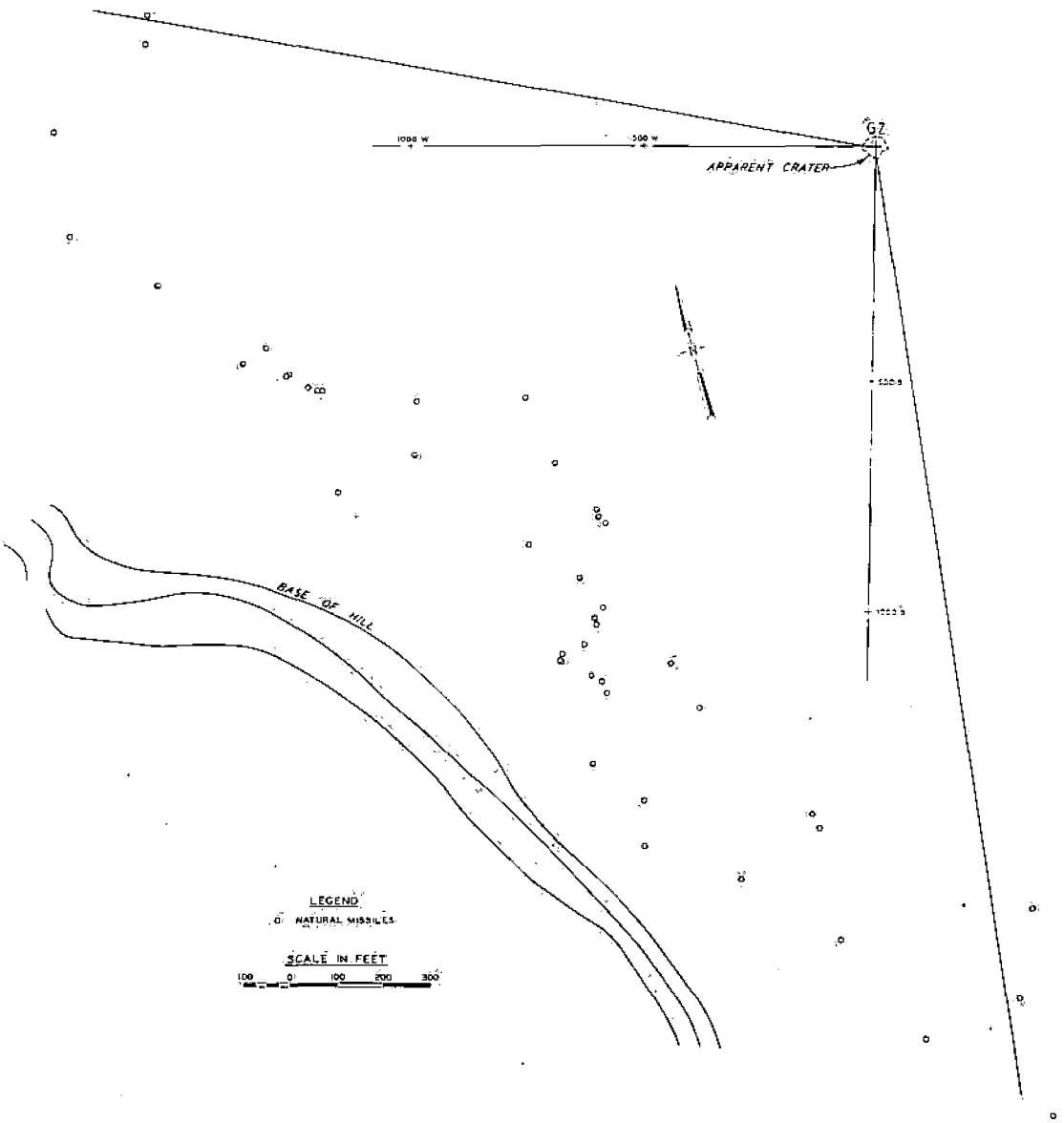

Figure 3.2 Outer limit of ejecta distribution, approximate southwest quadrant of MINE ORE.

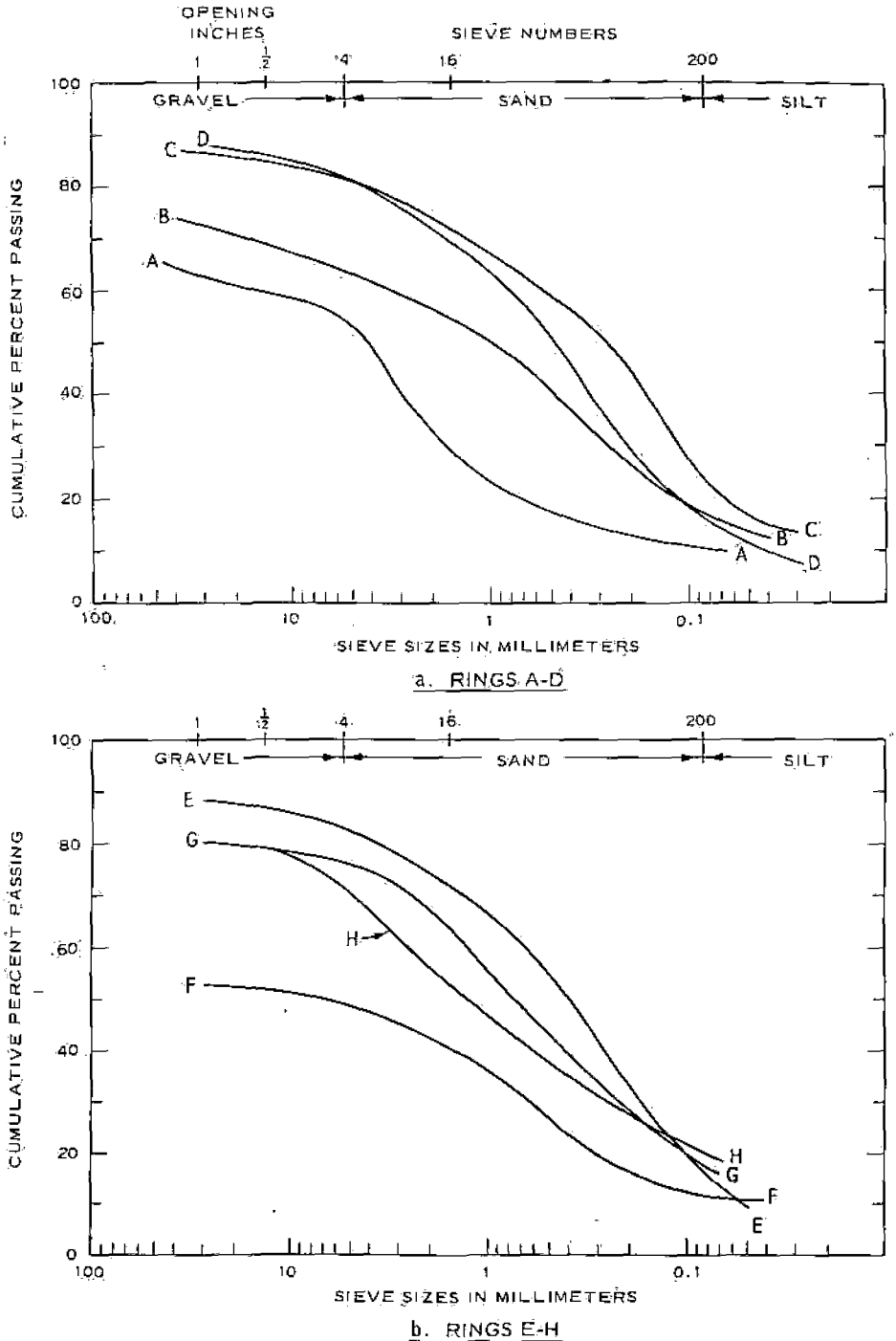

Figure 3.3 Grain-size distribution of ejecta dust, Rings A-H, MINE ORE.

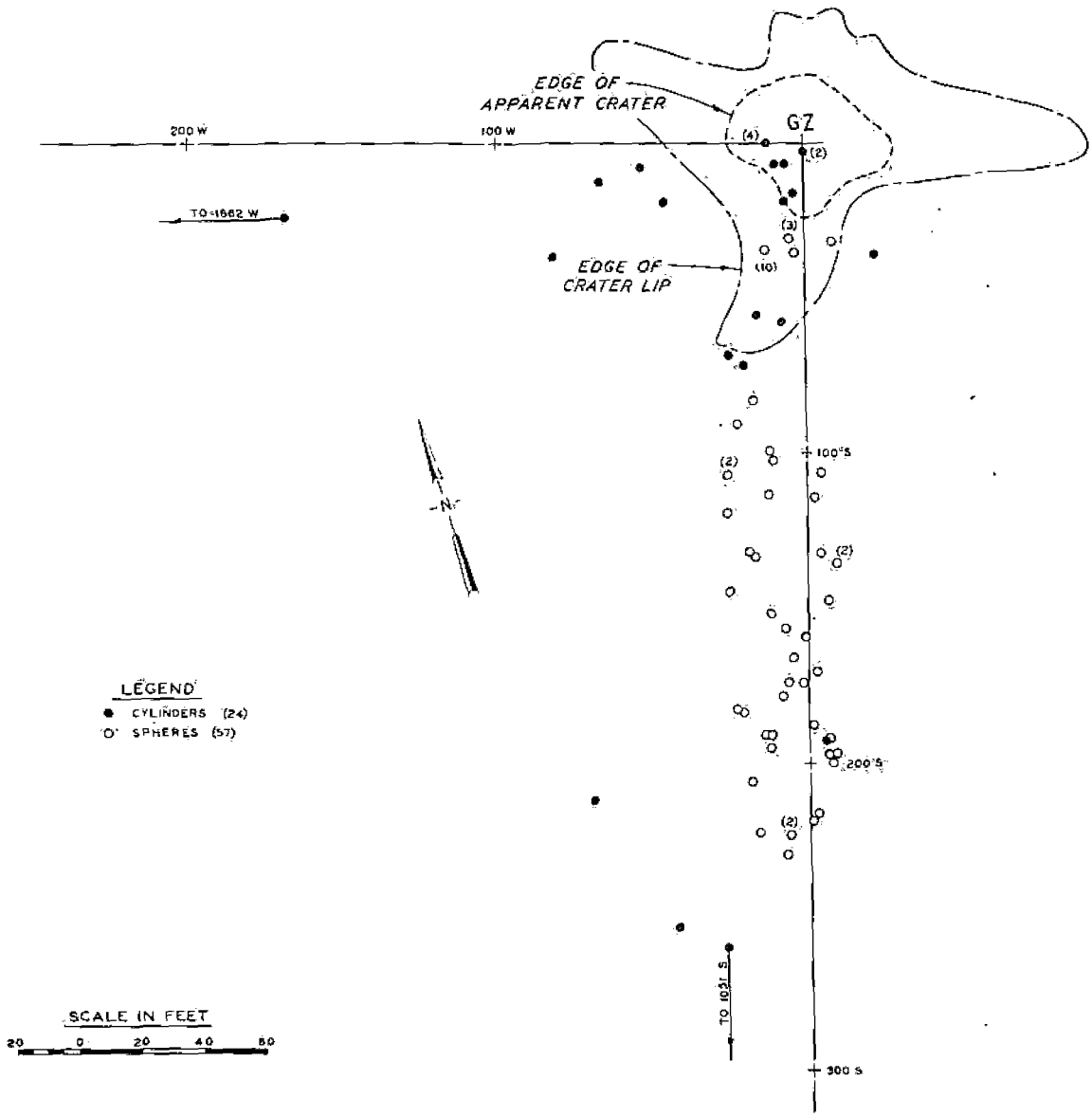

Figure 3.4 Postshot positions of artificial missiles, MINE ORE.

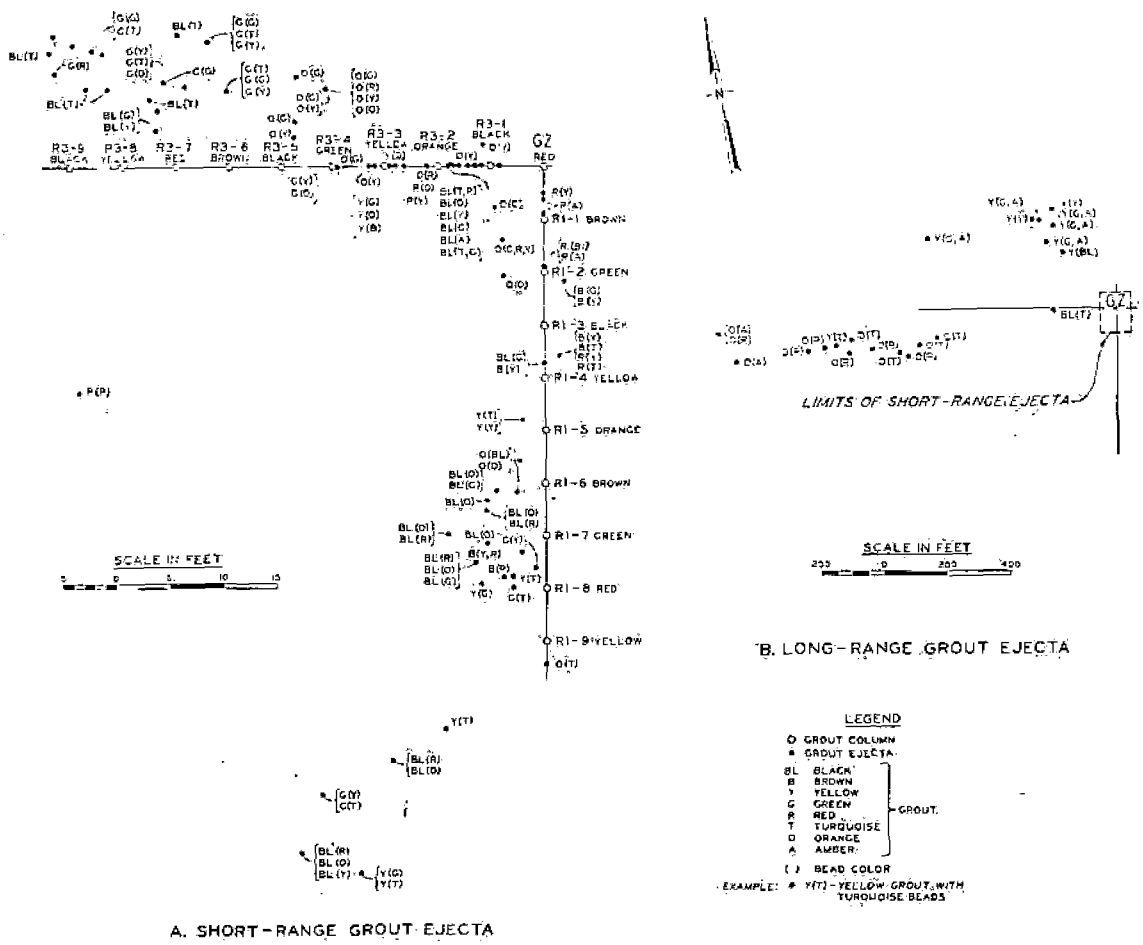

Figure 3.5 Postshot positions of colored-grout ejecta, MINE ORE.

Figure 3.6 MINE UNDER ejecta distribution, showing a partial plane-table survey of the larger (diameter ≥1 foot) natural missiles and the outer periphery of missiles at least 1 pound in weight.

CHAPTER 4

DISCUSSION OF RESULTS, MINE ORE EVENT

4.1 EJECTA MASS DENSITY, VOLUME, AND AZIMUTHAL DISTRIBUTION

The primary objective of this study was to obtain data on ejecta mass density and azimuthal distribution. The test procedures used to fulfill this objective (collector pads; camera, mount, and grid; counting sectors) provided good information on the larger particles, but were of doubtful value with regard to the finer particles (say 1/2 inch or less), especially beyond the C or D rings.

Figure 4.1 shows graphically the areal mass density plotted as a function of radial distance from GZ. The density data in this plot include those obtained from the lip excavation, photographic techniques, and the counting sectors. Data for the crater lip and south and west radials have been fitted to straight lines on logarithmic paper by the method of least squares. Additionally, an average, overall fit of the data is presented. It compares favorably with the distribution observed in other explosion tests in rock or cohesive-type materials (References 5, 12, and 13), especially when differences in shot geometry are taken into consideration. From the equation for average areal distribution, the total weight of ejected material E_w can be calculated as follows:

$$E_w = 2\pi \int_{r_a}^{\infty} \delta R \, dR \qquad (4.1)$$

(for notation, see Figures 1.1 and 4.1). The lower limit is taken to correspond with the average crater radius, although the distance r_h is theoretically correct. For crater and lip shapes like those of the MINE ORE Event, the error thus incurred is considered negligible. Similarly, experience has shown that the integration may be carried to infinity without significantly affecting results. Substituting,

$$E_W = 6.28 \int_{23}^{\infty} \left(3.90 \times 10^6 \, R^{-2.95}\right) R \, dR$$

$$= 1.32 \times 10^6 \text{ pounds}$$

The volume of ejecta, based upon the assumption of granitic density of 162 pcf and making no allowances for bulking, is found to be approximately 300 yards^3, probably significant to only the first integer.

An examination of the ejecta data from the photographic stations and counting sectors showed no clear relation between mean ejecta size and radial distance. However, these covered a small fraction of the total area, and an overall, visual survey showed a decrease in both size and missile numbers with increasing radial distance. This was particularly evident in the ejecta rays. The mean equivalent diameter for a piece of ejecta beyond the crater lip was about 3 inches. The average size in the sampled area of the crater lip (Figure 2.3) was between 6 and 12 inches, based upon the sieve-analysis

data in Table 3.1. The maximum-size particle ejected beyond the crater lip had an equivalent diameter of about 3 feet. It was located approximately 260 feet northwest of GZ. The largest particle in the crater lip was about 5 by 4 by 2-1/2 feet (about 3,100 pounds) located in Sector 3 of Radial 4 (Figure 2.3).

The most striking feature of the azimuthal distribution in this experiment was the pronounced ejecta rays, both in the crater lip and beyond (Figure 3.1). These rays indicate the strong dependence of ejecta distribution in rock on the site geology. The most influential factor in this distribution was the jointing pattern of the rock; comparison of ejecta-ray orientation and direction of major rock jointing in the crater (Figure 4.2) showed that the rays were very nearly parallel to major rock-joint faces. A specific example was the scarcity of ejecta directly north of GZ. A large vertical joint face north of GZ apparently deflected practically all of the ejecta originally traveling in a northerly direction into the northwest and east rays. All of the major ejecta rays can thus be traced to parallel joint faces within the crater area (Reference 11). Azimuthal distribution is illustrated graphically in Figure 4.3. For this purpose, data from close-in (Rings A-D) collector pads have been included with those from other sources.

4.2 EJECTA MISSILE RANGES

The range of maximum ejecta distances which might be expected

from the calculations in Chapter 1 is around 1,000 to 4,000 feet. This wide variation reflects the uncertainty concerning the origin of the ejection process. Calculations based upon a scouring action by the shock front provide the lower limit of maximum-distance predictions. The most promising approach to determination of ejecta ranges would appear to be by scaling according to charge yields, but here the choice of scaling exponents produces a wide variation of results. In addition to the factors discussed in Chapter 1, there were a number of physical characteristics of the site which may have affected scaling relations between the calibration series and MINE ORE, such as joint pattern, rock competence, and the various topographical features. Further, more detailed data will probably be necessary to establish a workable scaling exponent for this particular geometry; based upon the MINE SHAFT data now available, it appears certainly to lie in the range of $W^{1/4}$ to $W^{1/3}$, and at this point conforms very well with $W^{0.3}$.

The range within which 90 percent of ejected material falls is a useful figure, since it denotes the limit of an area within which the missile population is relatively dense. Based on weight, the 90 percent ejecta limit (or any desired limit) may be calculated from Equation 4.1. Again using the average curve from Figure 4.1,

$$E_{W_{90}} = 6.28 \int_{23}^{R_{90}} \left(3.90 \times 10^{6} R^{-2.95}\right) R \, dR$$

where

$E_{w_{90}}$ = 90 percent of the total weight of ejecta and

R_{90} = the 90 percent limit of ejected material

Thus

$$(0.90)(1.32 \times 10^6) = 2.45 \times 10^7 \left[\frac{R_{90}^{-0.95}}{-0.95} - \frac{(23)^{-0.95}}{-0.95} \right]$$

and

$$R_{90} = 263 \text{ feet}$$

Similar calculations can be made for debris falling beyond the crater lip. This was done for the south and west radials, using a lower limit of integration = 100 feet, and the results indicate that, on the average, 90 percent of the ejected material falling beyond the crater lip is contained within a radius of 1,375 feet.

4.3 SECONDARY EXPERIMENTAL OBJECTIVES

Between the grout-column and artificial-missile data, sufficient information was obtained to permit certain conclusions on the mechanics of the MINE ORE crater formation. This analysis is contained in Reference 11.

The definition of ejecta trajectories is largely dependent upon correlation of artificial-missile data with test photography. Additional time will be required to accomplish this secondary objective. Analysis of the test photography (Reference 14) has, however, provided

valuable data for this purpose. Ejecta speeds on the order of 600 ft/sec were observed upon emergence from the fireball. It is interesting to note that the velocity values reported in Reference 14 also indicate a scaling factor of approximately $W^{0.3}$. Ejection angles (with the horizontal) were very close to that assumed in Chapter 1. Unfortunately, camera failure precluded observation of much of the ejecta after about 2 seconds following detonation. Projections of the observed portions of these trajectories (in Reference 14) generally result in greater ranges than actually occurred, especially when the probable bounce and roll of the individual particles are considered. Although the middle and terminal portions of ejecta trajectories are still incompletely understood, it appears that an analysis of the photography and artificial-missile data, taking into consideration such external forces as afterwinds, may contribute to a solution of the problem.

The evaluation of natural missile hazards will also require more time than has been available for preparation of this report. The establishment of a usable scaling exponent for ejecta range is an important step in the realization of this objective, which must also include a statistical study of areal distribution for various particle sizes at various ranges.

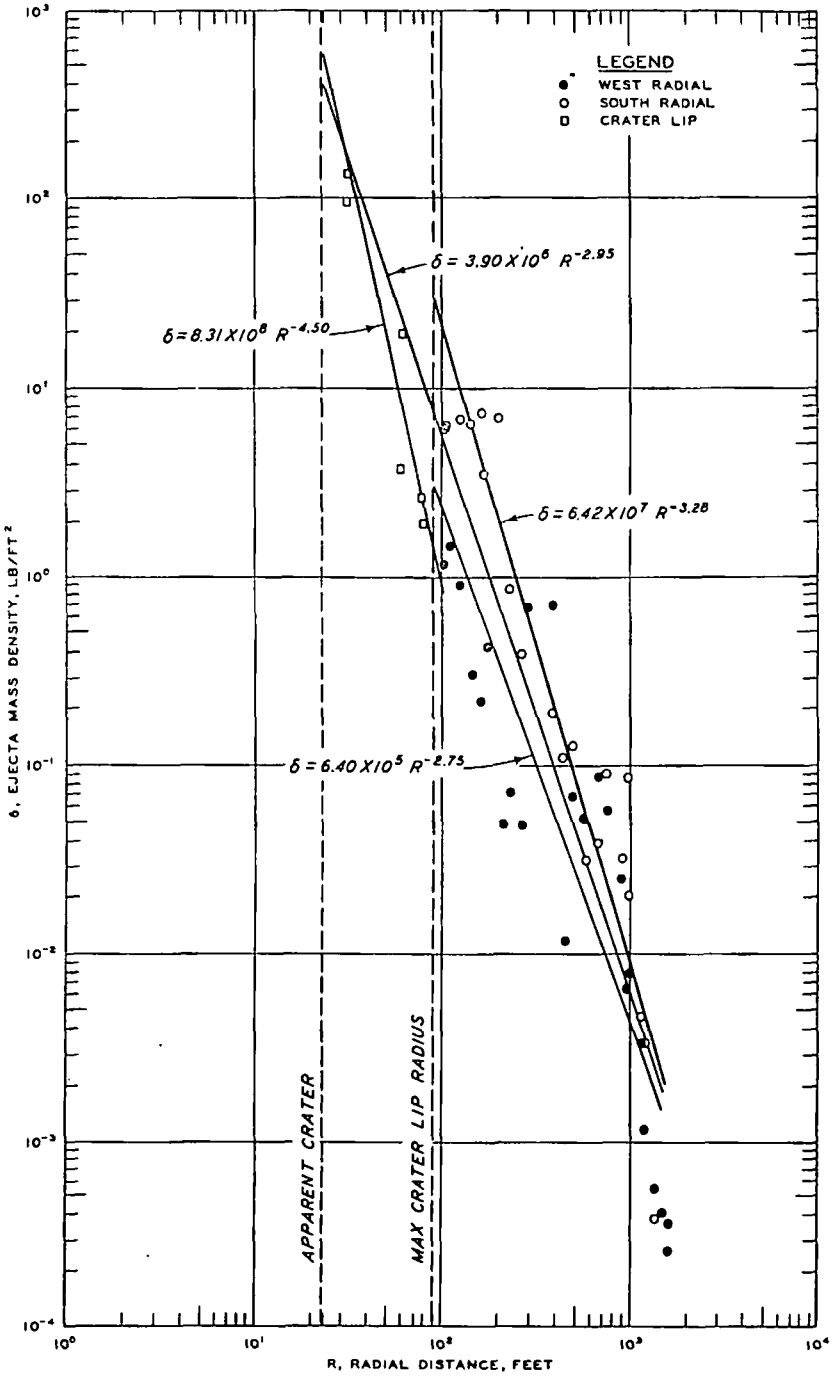

Figure 4.1 Areal mass density of ejecta as a function of distance from GZ, Event MINE ORE.

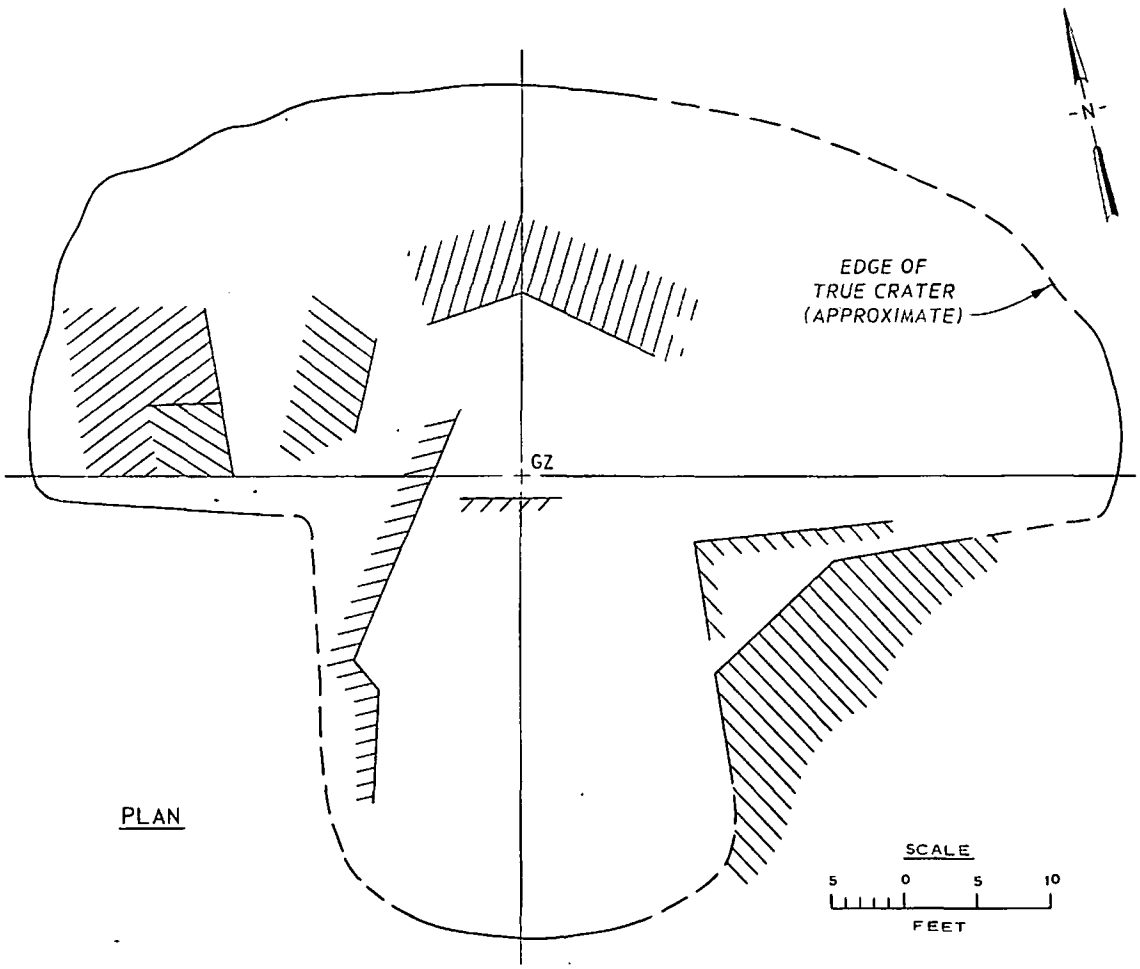

Figure 4.2 Rock-joint faces which affected MINE ORE ejecta distribution (Reference 11).

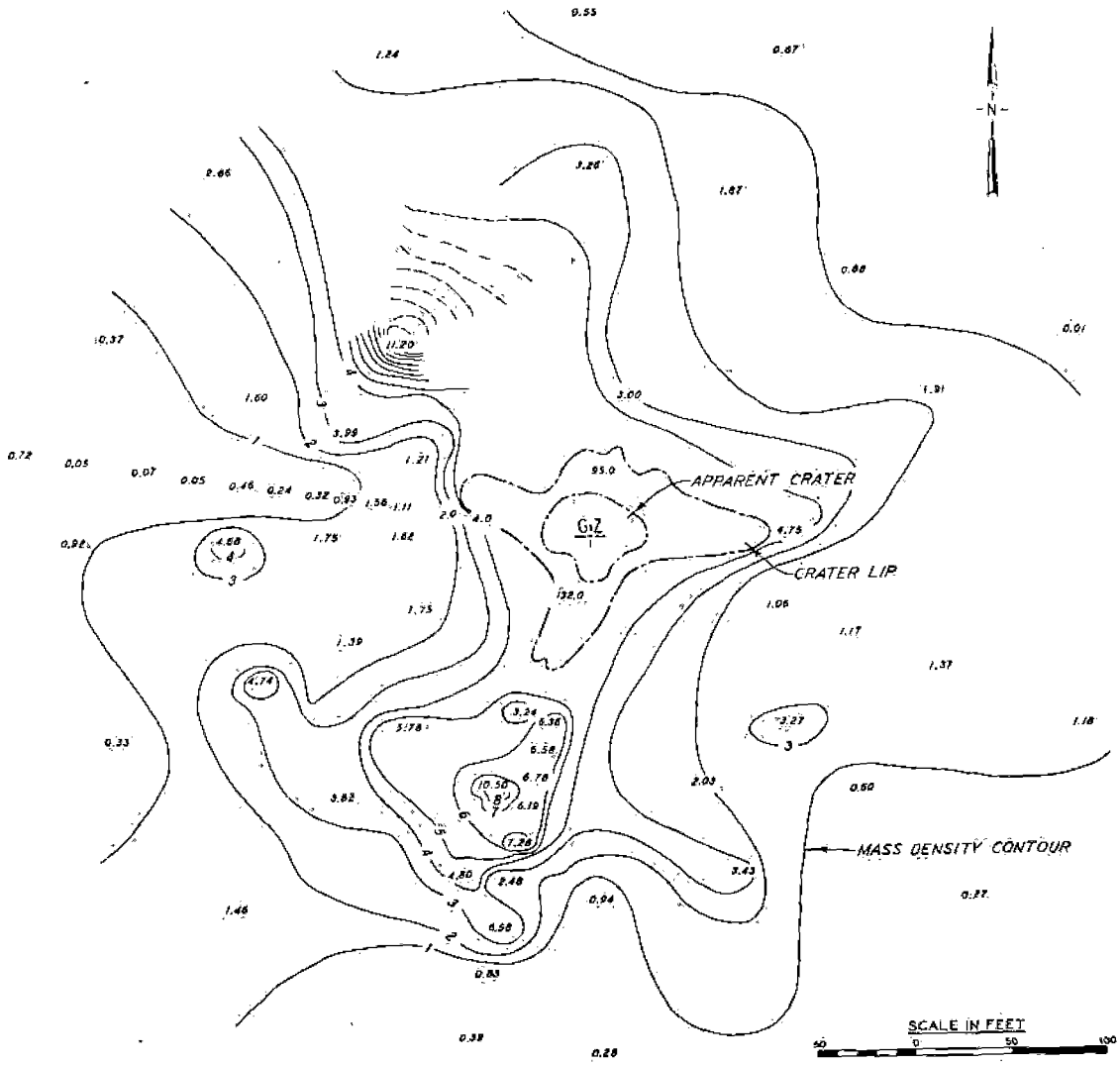

Figure 4.3 Isodensity contours, MINE ORE. Contours and data points represent areal densities of ejecta in pounds per square foot.

CHAPTER 5

TENTATIVE CONCLUSIONS AND RECOMMENDATIONS

5.1 TENTATIVE CONCLUSIONS

In view of the possibility of a second experiment in the MINE SHAFT Series essentially duplicating the MINE ORE Event,[1] firm conclusions regarding the ejecta studies should be delayed to include, if possible, considerations on the reproducibility of the data. Certain tentative conclusions can, however, be drawn on the basis of MINE ORE as follows:

1. Ejecta distribution from a surface or very near-surface burst in rock is highly dependent upon the joint pattern of the medium. The average azimuthal distribution as a function of range, however, does not differ markedly from those observed for other large explosions in rock or cohesive material and at deeper depths of burial (DOB's). It does differ from the distribution observed at or near optimum DOB (Reference 15).

2. Ejecta ranges for this experimental geometry scale according

---

[1] Memorandum from the Technical Director, MINE SHAFT Series, U. S. Army Engineer Waterways Experiment Station, Vicksburg, Mississippi; Subject: "Follow-On Events of the MINE SHAFT Series"; 19 November 1968; Unclassified.

to an exponent which is significantly larger than that indicated by theory. Lacking better data, this exponent may be taken as approximately $W^{0.3}$.

3. For the MINE ORE Shot, the missile hazard to exposed personnel would have extended to a maximum distance of around 2,200 to 2,400 feet. At this range, the hazard would have consisted mostly of small (less than 1 pound) ejecta particles bouncing along the ground, and in most cases breaking up on impact. For 1-pound particles, capable of doing considerable damage, the maximum danger range was slightly over 2,100 feet. Ejecta population was quite sparse at these ranges, however, and the hazard, in terms of the probability of a given spot being struck, was small.

5.2 RECOMMENDATIONS

5.2.1 Procedural Changes. The general approach to this experiment appears sound, and the authors recommend that it be repeated in essentially the same form on future events for which ejecta is expected. Several recommendations seem in order, however, as follows:

1. Increased "seeding" of the crater area with artificial missiles seems desirable, with the object of increasing the numbers of different sizes, shapes, and densities of those missiles which can be located postshot. Particular attention should be paid to the region

between the edge of the charge and two or three charge radii from GZ, as it appears that the greatest ranges may be realized by ejecta originating in this general area.

2. An increased effort to obtain early photography of ejected material is highly desirable, although the technical problems which this imposes are recognized. Further, it is recommended that an effort be made to photographically follow entire missile trajectories. There is evidence that debris which is ejected from a position near the charge has a high initial speed but slows to a much lower speed early in its trajectory (Reference 1). Further, it appears that afterwinds exert a varying drag force upon the longer range particles. More complete information on typical trajectory histories will probably be necessary to an understanding of observed ranges and size distributions.

3. Photographic sampling of ejecta was quite successful, and this procedure should be expanded to include more and larger samples.

4. The use of collector pads should be reduced or eliminated. This is one of the most time-consuming aspects of an experiment of this type, and one which yields probably the least usable data. In and near the crater lip, where deposition of fine particulate may be significant, prepared surfaces (e.g., asphalt) are recommended to replace the pads. Farther out, if dust-density data are required, a better sampling technique is needed. There appear to be two

possibilities--dust-cloud opacity measurements and aboveground vacuum samplers. It is recommended that both of these techniques be investigated for future experiments.

5.2.2 Postseries Analysis. Rigorous analysis of gathered ejecta data was not within the scope of the ejecta project as concerns the first two events of the MINE SHAFT Series.[2] Time has not permitted such a detailed study. It might rather be appropriate for such an analysis to await the completion of all ejecta-producing MINE SHAFT events. It is most important, however, that the experimenter be afforded the opportunity to completely analyze, correlate, and document an experiment before it is considered closed. This will provide the maximum in descriptive detail to the later user of the experimental input, with the least likelihood of misinterpretation or the necessity for laborious correlative effort in assessing the ejecta phenomena.

---

[2] See Paragraph 5.5, Reference 10.

REFERENCES

1. E. B. Ahlers and C. A. Miller; "Ferris Wheel Series, FLAT TOP Event, Project 1.5a, Crater Ejecta Studies"; POR-3006 (WT-3006), November 1966; Defense Atomic Support Agency, Washington, D. C.; Report prepared by Illinois Institute of Technology Research Institute, Chicago, Illinois; Unclassified.

2. J. Wisotski; "Photographic Data from Calibration MINE SHAFT Series, Interim Report Part I"; 3884-6806-I, June 1968; Denver Research Institute, University of Denver, Denver, Colorado; Unclassified.

3. A. D. Rooke and L. K. Davis; "Ferris Wheel Series, FLAT TOP Event, Project 1.9, Crater Measurements"; POR-3008 (WT-3008), August 1966; Defense Atomic Support Agency, Washington, D. C.; Report prepared by U. S. Army Engineer Waterways Experiment Station, CE, Vicksburg, Mississippi, and published as its Miscellaneous Paper No. 1-896; Unclassified.

4. A. E. Sherwood; "The Effect of Air Drag on Particles Ejected During Explosive Cratering"; UCRL-14974, June 1966; Lawrence Radiation Laboratory, Livermore, California; Unclassified.

5. A. D. Rooke, Jr., G. B. Clark, and J. N. Strange; "Operation

SUN BEAM, Shot JOHNIE BOY, Project 1.5, Mass Distribution Measurements (U)"; POR-2282 (WT-2282), 25 February 1965; Defense Atomic Support Agency, Washington, D. C.; Confidential.

6. G. P. Ganong and W. A. Roberts; "The Effect of the Nuclear Environment on Crater Ejecta Trajectories for Surface Bursts"; Technical Report No. AFWL-TR-68-125, October 1968; Air Force Weapons Laboratory, Kirtland Air Force Base, New Mexico; Unclassified.

7. L. K. Davis; "MINE SHAFT Series, Subtask N123, Calibration Cratering Events" (in preparation); U. S. Army Engineer Waterways Experiment Station, CE, Vicksburg, Mississippi; Unclassified.

8. A. J. Chabai; "Scaling Dimensions of Craters Produced by Buried Explosions"; SC-RR-65-70, February 1965; Sandia Corporation, Albuquerque, New Mexico; Unclassified.

9. L. J. Vortman; "Maximum Missile Ranges from Surface and Buried Explosions"; SC-RR-67-616, September 1967; Sandia Corporation, Albuquerque, New Mexico; Unclassified.

10. "MINE SHAFT Series, Events MINE UNDER and MINE ORE, Technical, Administrative, and Operational Plan"; DASIAC Special Report 77-1, 1 October 1968; Headquarters, Defense Atomic Support Agency, DASA Information and Analysis Center, General Electric Company,

TEMPO, Santa Barbara, California; Unclassified.

11. L. K. Davis; "MINE SHAFT Series, Events MINE ORE and MINE UNDER, Subtask N121, Crater Investigations" (in preparation); U. S. Army Engineer Waterways Experiment Station, CE, Vicksburg, Mississippi; Unclassified.

12. M. V. Anthony, T. P. Day, and C. R. Wauchope; "FERRIS WHEEL Series, FLAT TOP Event, Project 1.5b, Ejecta Distribution from FLAT TOP I Event"; POR-3007 (WT-3007), 18 October 1965; Defense Atomic Support Agency, Washington, D. C.; Report prepared by the Boeing Company, Seattle, Washington; Unclassified.

13. A. D. Rooke, Jr., and T. D. Chew; "Crater and Ejecta Measurements for a Full-Scale Missile Detonation in an Underground Cell"; Miscellaneous Paper No. 1-853, November 1966; U. S. Army Engineer Waterways Experiment Station, CE, Vicksburg, Mississippi; For Official Use Only.

14. J. Wisotski; "Technical Photography from MINE UNDER and MINE ORE Events of the MINE SHAFT Series"; 3884-6902-F, February 1969; Denver Research Institute, University of Denver, Denver, Colorado; Unclassified.

15. L. K. Davis and A. D. Rooke, Jr.; "DANNY BOY Event,

Project 1.6: Mass Distribution Measurements of Crater Ejecta and Dust; POR 1815 (WT), Appendix B, Volumetric Equalities of the Crater"; Miscellaneous Paper No. 1-754, December 1965; U. S. Army Engineer Waterways Experiment Station, CE, Vicksburg, Mississippi; Unclassified.

DISTRIBUTION LIST

Address	No. of Copies
DOD	
Director, Defense Atomic Support Agency, Washington, D. C. 20305 ATTN: Technical Library (APTL); STSP; OAOP (OPQR)	5
Commander, Field Command, Defense Atomic Support Agency, Sandia Base, Albuquerque, N. Mex. 87115 ATTN: Technical Library (FCTG-5; FCDV-1)	3
Commander, Test Command, Defense Atomic Support Agency, Sandia Base, Albuquerque, N. Mex. 87115 ATTN: Document Control	2
Administrator, Defense Documentation Center, Cameron Station, Bldg. 5, Alexandria, Va. 22314 ATTN: Document Control	20
Director, Defense Intelligence Agency, Washington, D. C. 20301 ATTN: DIAAP-8B; DIAST-3	2
Assistant to the Secretary of Defense (Atomic Energy), Washington, D. C. 20315 ATTN: Class Rec. Library	1
Director of Defense Research and Engineering, Washington, D. C. 20301 ATTN: Asst. Director (Strategic Weapons); Asst. Director (Nuclear Programs)	2
Director, Weapons Systems Evaluation Group, Washington, D. C. 20305 ATTN: Document Control	1
Joint Strategic Target Planning Staff, Offutt AFB, Nebr. 68113	1
Army	
Chief of Engineers, Department of the Army, Bldg. T-7, Gravelly Point, Washington, D. C. 20315 ATTN: ENGMC-EM; ENGME; Director of Military Construction	4
Chief of Research and Development, Department of the Army, Washington, D. C. 20310 ATTN: Nuclear, Chemical-Biological Division	1
Commanding General, Army Engineer Center, Ft. Belvoir, Va. 22060 ATTN: Asst. Commandant Engineer School	1
Commanding Officer, Army Combat Developments Command, Institute of Nuclear Studies, Ft. Bliss, Tex. 79916 ATTN: Document Control	1
Commanding Officer, Army Engineer Nuclear Cratering Group, Lawrence Radiation Laboratory, P. O. Box 808, Livermore, Calif. 94550 ATTN: Document Control	1
Division Engineer, Army Engineer Division, Ohio River, P. O. Box 1159, Cincinnati, Ohio 45201 ATTN: Document Control	1
Division Engineer, Army Engineer Division, Huntsville, Box 1600 West Station, Huntsville, Ala. 35807 ATTN: Mr. H. L. Solomonson; Mr. M. Dembo	2
District Engineer, Army Engineer District, Omaha, 215 N. 17th Street, Omaha, Nebr. 68102 ATTN: Document Control	1

Address	No. of Copies
Army (Continued)	
Commanding General, Army Materiel Command, Bldg. T-7, Gravelly Point, Washington, D. C. 20315 ATTN: AMCRD-BN	2
Commanding Officer, Army Ballistic Research Laboratories, Aberdeen Proving Ground, Md. 21005 ATTN: Document Control for Mr. John Keefer	2
Navy	
Chief of Naval Operations, Navy Department, Washington, D. C. 20350 ATTN: OP-03EG; OP-75	3
Chief of Naval Research, Navy Department, Washington, D. C. 20360 ATTN: Code 811	1
Commander, Naval Facilities Engineering Command, Headquarters, Washington, D. C. 20390 ATTN: Code 04; Code 03	2
Commander, Naval Ship Engineering Center, Washington, D. C. 20360 ATTN: Document Control	1
Director, Strategic Systems Projects Office, Navy Department, Washington, D. C. 20360 ATTN: NSP-272	1
Commanding Officer and Director, Naval Civil Engineering Laboratory, Port Hueneme, Calif. 93041 ATTN: Document Control	1
Commander, Naval Ordnance Laboratory, Silver Springs, Md. 20910 ATTN: EA; EU; E	3
Superintendent, Naval Postgraduate School, Monterey, Calif. 93940 ATTN: Technical Library	1
Commanding Officer, Naval School, Civil Engineer Corps Officers, Naval Construction Battalion Center, Port Hueneme, Calif. 93041 ATTN: Document Control	1
Commanding Officer and Director, Naval Ship Research and Development Center, Washington, D. C. 20007 ATTN: Technical Library	1
Air Force	
Headquarters, USAF, Washington, D. C. 20330 ATTN: AFNINDE (Dissemination Req. Res. Br.); AFOCE (Dir. of Civil Eng.); AFRDQSN (Strat. and Def. Forces, Nuc Ord. Div.); AFRDDF (Missile Sys. Div., Dir. of Dev.)	4
Headquarters, Air Force Systems Command, Andrews AFB, Washington, D. C. 20331 ATTN: SCS-7 (COL W. P. Wood); SCTSW	2
Strategic Air Command, Offutt AFB, Nebr. 68113 ATTN: OAI (Stinfo Section); DPLBIC (LTC J. B. Tye)	2
AFSC STLO (SCTL-10), Air Force UPO, Los Angeles, Calif. 90045 ATTN: RTSAL	1

Address	No. of Copies
Air Force (Continued)	
Air Force Weapons Laboratory, AFSC, Kirtland AFB, N. Mex. 87117 ATTN: WLIL, Technical Library; WLDC; WLPM; Dr. E. Zwoyer	4
Aerospace Defense Command, Ent AFB, Color 80912 ATTN: ADLDC (DCS OF Plans); ADLMD-W (Missile and Space Weapons Div.)	4
Space and Missile Systems Organization, AFSC, Air Force Unit Post Office, Los Angeles, Calif. 90045 ATTN: SMNP; SAFSP-6	4
Space and Missile Systems Organization, AFSC, Norton AFB, Calif. 92409 ATTN: SMQHF; SMQN (MINUTEMAN Engineering Div.); SMTSM-1; SMY	7
AEC	
Sandia Corporation, P. O. Box 5800, Albuquerque, N. Mex. 87116 ATTN: Document Control for: Dr. M. L. Merritt, Mr. W. R. Perrett	3
Other	
Bureau of Mines, Bldg. 20, Denver Federal Center, Denver, Colo. 80225 ATTN: Science Advisor, Mining Research, Dr. L. A. Obert	1
Civilian Contractors	
Aerospace Corporation, P. O. Box 95085, Los Angeles, Calif. 90045 ATTN: Technical Information Services	2
Aerospace Corporation, 1111 East Mill Street, P. O. Box 1308, San Bernardino, Calif. 92402 ATTN: Mr. Mason Watson; Mr. W. Pferrerle; Mr. Craig Smith; Dr. William Brown	4
Agbabian-Jacobsen Associates, 8939 South Sepulveda Blvd., Los Angeles, Calif. 90045 ATTN: Document Control	1
Analytical Services, Inc., 5613 Leesburg Pike, Falls Church, Va. 22041 ATTN: George Hesselbacher	1
Applied Theory, Inc., 1728 Olympic Blvd., Santa Monica, Calif. 90404 ATTN: Security Officer	1
Battelle Memorial Institute, 505 King Avenue, Columbus, Ohio 43201 ATTN: Mr. R. W. Klingesmith	1
The Boeing Company, P. O. Box 3707, Seattle, Wash. 98124 ATTN: Mr. John Blaylock	1
EG&G, Inc., P. O. Box 227, Bedford, Mass. 01730 ATTN: Document Control Center for D. W. Hansen	1
Engineering Physics Company, 12721 Twinbrook Parkway, Rockville, Md. 28052 ATTN: Mr. Vincent J. Cushing	1
Environmental Research Corporation, 813 N. Royal Street, Alexandria, Va. 22314 ATTN: Mr. O. A. Israelson	1

Address	No. of Copies
Civilian Contractors (Continued)	
General American Research Division, General American Transportation Corp., 7449 N. Natchez Avenue, Niles, Ill. 60648 ATTN: Dr. Neidhardt	1
General Electric Company, Tempo-Center for Advanced Studies, 816 State Street, Santa Barbara, Calif. 93102 ATTN: DASA Information and Analysis Center, W. Chan	2
General Motors Corporation, Manufacturing Development, Manufacturing Staff, 12 Mile and Mound Roads, Warren, Mich. 48092 ATTN: Mr. W. Isbell; Dr. C. Maiden	2
General Research Corporation, P. O. Box 3587, Santa Barbara, Calif. 93105 ATTN: Dr. Benjamin Alexander	1
General Research Corporation, 1501 Wilson Blvd., Arlington, Va. 22209 ATTN: Dr. W. Layson	1
Gulf General Atomic, Inc., P. O. Box 1111, San Diego, Calif. 92112 ATTN: Chief, Tech. Information Services for: H. Kratz	1
IIT Research Institute, 10 West 35th Street, Chicago, Ill. 60616 ATTN: Technical Library; Dr. E. Sevin	2
Institute for Defense Analyses, 400 Army-Navy Drive, Arlington, Va. 22202 ATTN: Technical Information Office	2
Kaman Sciences Corporation, Kaman Nuclear Division, Garden of the Gods Road, Colorado Springs, Colo. 80907 ATTN: Mr. Paul Ellis	1
Dr. Nathan M. Newmark, 1114 Civil Engineering Bldg., University of Illinois, Urbana, Ill. 61801 ATTN: Professor D. V. Deere; Professor A. J. Hendron	2
Physics International Company, 2700 Merced Street, San Leandro, Calif. 94577 ATTN: Dr. Charles Gadfrey	1
The Rand Corporation, 1700 Main Street, Santa Monica, Calif. 90406 ATTN: Library; Dr. A. L. Latter; Dr. H. Brode; Mr. W. B. Wright; Dr. Olen A. Nance; Dr. C. C. Mow	6
Research Analysis Corporation, McLean, Va. 22101 ATTN: Documents Library	1
Stanford Research Institute, 333 Ravenswood Avenue, Menlo Park, Calif. 94025	1
Systems, Science, and Software, Inc., P. O. Box 1620, La Jolla, Calif. 92037 ATTN: Document Control	1
TRW Systems Group, San Bernardino Operations, P. O. Box 1310, 600 East Mill Street, San Bernardino, Calif. 92402 ATTN: J. L. Merritt, Mgr. HARD ROCK SILO OFF.; Mr. Fred Pieper	2
TRW Systems Group, One Space Park, Redondo Beach, Calif. 90278 ATTN: Mr. J. Carpenter	1

Address	No. of Copies
Civilian Contractors (Continued)	
URS Corporation, 1811 Trousdale Drive, Burlingame, Calif. 94011 ATTN: Mr. Harold Mason	1
Paul Weidlinger, Consulting Engineer, 777 Third Avenue, New York, N. Y. 10017 ATTN: Dr. M. Baron	1
U. S. Geological Survey, Flagstaff, Ariz. 86001 ATTN: Dr. Roddy	1
Defence Research Establishment, Suffield, Ralston, Alberta, Canada ATTN: Mr. A. P. R. Lambert	1
Denver Research Institute, University of Denver, University Park, Denver, Colo. 80210 ATTN: Mr. John Wisotski	1

Unclassified
Security Classification

DOCUMENT CONTROL DATA - R & D

(Security classification of title, body of abstract and indexing annotation must be entered when the overall report is classified)

1. ORIGINATING ACTIVITY (Corporate author)
U. S. Army Engineer Waterways Experiment Station
Vicksburg, Mississippi

2a. REPORT SECURITY CLASSIFICATION
Unclassified

2b. GROUP

3. REPORT TITLE
MINE SHAFT SERIES: EVENTS MINE UNDER AND MINE ORE, EJECTA STUDIES

4. DESCRIPTIVE NOTES (Type of report and inclusive dates)
Final report

5. AUTHOR(S) (First name, middle initial, last name)
John W. Meyer
Allen D. Rooke, Jr.

6. REPORT DATE	7a. TOTAL NO. OF PAGES	7b. NO. OF REFS
September 1969	91	16

8a. CONTRACT OR GRANT NO.	9a. ORIGINATOR'S REPORT NUMBER(S)
b. PROJECT NO.	Miscellaneous Paper N-69-2
c.	9b. OTHER REPORT NO(S) (Any other numbers that may be assigned this report)
d.	

10. DISTRIBUTION STATEMENT
Each transmittal of this document outside the Department of Defense must have prior approval of Defense Atomic Support Agency.

11. SUPPLEMENTARY NOTES	12. SPONSORING MILITARY ACTIVITY
	Defense Atomic Support Agency Washington, D. C.

13. ABSTRACT

The MINE SHAFT Series is a program of high-explosive tests primarily concerned with ground-shock and cratering effects from explosions at or near the surface of a rock medium. The series is sponsored by the Defense Atomic Support Agency (DASA) as a follow-on to similar tests in soil (SNOW BALL, DISTANT PLAIN, PRAIRIE FLAT). The two major events of MINE SHAFT during 1968 were MINE UNDER and MINE ORE; both were explosions of 100-ton TNT spheres detonated in near-surface geometries and in/over a granite medium. Studies of the crater ejecta were conducted on MINE ORE (buried one-tenth of the charge radius) with the objectives of determining the spoil density and distribution from this event, examining the role of the ejection mechanism in crater formation for this medium, and obtaining additional information on natural missile trajectories. MINE UNDER, an above-surface event, produced a spalled rubble mound and a small field of debris; this was also recorded as part of the study. MINE ORE produced a low, irregular crater lip which extended to an average range of 47 feet from ground zero (GZ) with a maximum of roughly 90 feet. Beyond this, discrete ejecta particle size and distribution frequency decreased with increasing distance from GZ. The maximum observed range was 2,120 feet for a 1-pound natural missile with smaller fragments found out to about 2,300 feet from GZ. Maximum ejecta ranges were observed downhill from and parallel to the main joints. Missile ranges scaled approximately as $W^{0.3}$. The jointing system of the rock appeared to be the single most influential element in concentrating debris along certain radials, as well as in the overall distribution of debris.

DD FORM 1 NOV 1473 REPLACES DD FORM 1473, 1 JAN 64, WHICH IS OBSOLETE FOR ARMY USE.

Unclassified
Security Classification

14. KEY WORDS	LINK A		LINK B		LINK C	
	ROLE	WT	ROLE	WT	ROLE	WT
Cratering						
Crater ejecta						
Ejection						
Explosions						
Ground shock						
Mine Ore (Event)						
Mine Shaft (Series)						
Mine Under (Event)						